Structural Chemistry
https://doi.org/10.1007/s11224-022-02066-z

REVIEW ARTICLE

An integrated computational approach towards the screening of active plant metabolites as potential inhibitors of SARS-CoV-2: an overview

Susankar Kushari[1,2] · Iswar Hazarika[1,3] · Damiki Laloo[1,4] · Suman Kumar[1,2] · Jun Moni Kalita[1,2] · Himangshu Sarma[5,6]

Received: 19 June 2022 / Accepted: 22 September 2022

Abstract

COVID-19 and its causative organism SARS-CoV-2 paralyzed the world and was designated a pandemic by the World Health Organization in March 2020. The worldwide health system is trying to discover an effective therapeutic measure since no clinically authorized medications are present. Screening of plant-derived pharmaceuticals may be a viable technique to fight COVID-19 in this vital situation. This review discusses the potential application of in silico approaches in developing new therapeutic molecules related to preventing SARS-CoV-2 infection. Also, it describes the binding affinity of various phytoconstituents with distinct SARS-CoV-2 target sites. In this perspective, an extensive literature survey was carried out to find the potential phytoconstituents to develop new therapeutic entities to treat COVID-19 in different online academic databases and books. Data retrieved from databases were analyzed and interpreted to conclude that many phytochemicals will bind with the 3-chymotrypsin-like (3CLpro) and papain-like proteases (PL^{pro}), spike glycoprotein, ACE-2, NSP15-endoribonuclease, and E protein targets of SARS-CoV-2 main protease using in silico molecular docking approach. The present investigations reveal that phytoconstituents such as curcumin, apigenin, chrysophanol, and gingerol are significantly binding with spike glycoprotein; laurolistine, acetoside, etc. are bound with M^{pro} for anti-SARS-CoV-2 therapies. Using virtual applications of in silico studies, the current study constitutes a progressive data analysis on the mechanism of binding efficiency of distinct classes of plant metabolites against the active sites of SARS-CoV-2. Furthermore, the current review also demonstrates the fundamental necessity of the alternative and complementary medicine for future therapeutic uses of phytoconstituents by phytochemists in the fight against COVID-19.

Keywords COVID-19 · In silico docking · Phytoconstituents · SARS-CoV-2

Abbreviations

ACE-2	Angiotensin-converting enzyme-2
$3CL^{pro}$	3-Chymotrypsin-like protease
COVID-19	Coronavirus disease 2019
CSF	Cerebrospinal fluid
EGCG	Epigallocatechin gallate
E protein	Envelope protein
FDA	Food and Drug Administration

✉ Damiki Laloo
damiki.laloo@gmail.com

✉ Himangshu Sarma
himangshu.amc@gmail.com

[1] Assam Science and Technology University, Guwahati-781013, Assam, India

[2] Department of Pharmaceutical Chemistry, Girijananda Chowdhury Institute of Pharmaceutical Science, Guwahati-781017 Assam, India

[3] Department of Pharmacology, Girijananda Chowdhury Institute of Pharmaceutical Science, Guwahati-781017 Assam, India

[4] Phytochemical Research Laboratory, Department of Pharmacognosy, Girijananda Chowdhury Institute of Pharmaceutical Science, Guwahati-781017 Assam, India

[5] Sophisticated Analytical Instrument Facility (SAIF), Girijananda Chowdhury Institute of Pharmaceutical Science, Guwahati-781017 Assam, India

[6] Department of Pharmaceutical Sciences, Faculty of Science & Engineering, Dibrugarh University, Dibrugarh-784006, Assam, India

Published online: 01 October 2022

HBA	Hydrogen bond acceptor
HBD	Hydrogen bond donor
HCoV	Human coronavirus
MERS-CoV	Middle East Respiratory Syndrome coronavirus
M^{pro}	Main protease
M protein	Membrane protein
mRNA	Messenger ribonucleic acid
N protein	Nucleocapsid protein
PDB	Protein data bank
PL^{pro}	Papain-like protease
RNA	Ribonucleic acid
RdRp	RNA-dependent RNA polymerase
SARS-CoV-2	Severe acute respiratory syndrome coronavirus 2
S protein	Spike protein
S-RBD	Spike protein receptor-binding domain
WHO	World Health Organization

Introduction

Among the two coronavirus subtypes (alpha and beta), beta coronavirus has been reported to be the major cause of three pathogenic zoonotic disease outbreaks over the last two decades. Severe acute respiratory syndrome coronavirus (SARS-CoV-2), Middle East respiratory syndrome coronavirus (MERS-CoV), and coronavirus disease 2019 (COVID-19) were epidemics in 2002, 2012, and 2019 [1]. COVID-19 caused havoc and damage to the world population and is a global threat in the twenty-first century [2]. This pandemic outbreak of COVID-19 will forever remain an unprecedented epidemic in the history of mankind [3]. As of April 20, 2022, the World Health Organization (WHO) had received reports of 504,079,039 confirmed COVID-19 cases worldwide, with reported deaths accounting for 6,204,155 [4]. Even though the race for eradicating the virus has been in extreme progress with the emergence of novel COVID-19 vaccines, biotechnological products, and antiviral drugs, however, scientists from all over the world are still trying to research the best possible diagnostic methods to put an end to this deadly pandemic.

Plants have been a source of medicine and food for ages [5, 6]. Around 80% of the world's population still relies on plants for their health [7]. Metabolites of the plant can be a potent source of alternative therapy for COVID-19 treatment [8]. In silico studies can be useful therapeutic tools to discover novel molecules as potential inhibitors of SARS-CoV-2, and this can be purpose by screening the binding efficacy of the plants' secondary metabolites against the active sites of the target proteins. Hence, the present review aims to specifically report the importance of in silico studies taking into account the binding efficacy of the active phytochemical compounds (isolated from plants) towards the active sites of SARS-CoV-2.

Methodology

The systematic review was performed as per PRISMA guidelines [9]. A literature survey was performed in "PubMed" using the indexed term (*in-silico* studies, phytoconstituents, and SARS-CoV-2) separated by Boolean operators ("AND" and "OR"), and a total of 233 articles were obtained. All the research articles and reviews published until February 7, 2022, were considered for the study. Exclusion criteria omitted from the investigation were in silico data for semi-synthetic derivatives and plant extracts. The phytoconstituents obtained from the review were further determined for their drug-likeness using the Molsoft database (www.molsoft.com/mprop/).

Results

Potential protein targets of SARS-CoV-2

The genome of SARS-CoV-2 consists of a 5′ untranslated region, which includes a 5′ leader sequence; an open reading frame encoding non-structural proteins; four structural proteins, which include spike (S), envelope (E), membrane (M), and nucleocapsid (N); several accessory proteins; and a 3′ untranslated region as shown in Fig. 1 [10]. These proteins can be targeted and used to develop a new drug. The protein targets of SARS-CoV-2 are explained in the following subsections for a better understanding of the drug effect.

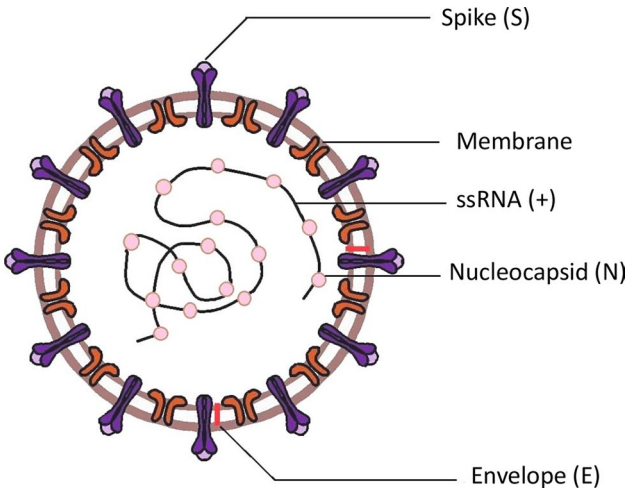

Fig. 1 Different binding epitopes for a drug target sites of SARS-CoV-2

Spike glycoprotein of SARS-CoV-2

The spike glycoprotein is the only structural protein responsible for the SARS- "crown"-like-CoV-2's structure; hence, the moniker "coronavirus" was coined. It is a transmembrane protein located in the outer region of the virus. The attachment of the spike glycoprotein to the host cell angiotensin-converting enzyme-2 receptor (ACE-2) is the first step in getting CoV into the host cells. The type II transmembrane serine protease on the host cell's surface clears ACE-2 and activates the receptor connected to spike-like S proteins. Virus entrance into cells is enabled by the conformational change that happens after activation. As a result, both type II transmembrane serine protease and ACE-2 are essential for viral entry. Homotrimers are generated when S protein protrudes from the viral surface, allowing enveloped viruses to adhere to host cells through ACE-2 attraction [10]. The cleavage of spike protein using proteases produces two subunits S1 and S2. Both the units play a major role in recognizing receptors and membrane fusion. Moreover, S1 is further divided into two important domains—the N-terminal domain and the C-terminal domain. The S1 C-terminal domain shows a higher affinity to bind with the ACE-2 receptor, contrary to the N-terminal domain. The receptor-binding domain of SARS-CoV-2 has been discovered to be the major area interacting with human ACE-2 [11]. The fusion peptide, a secondary proteolytic site, two heptad-repeat domains preceding the transmembrane domain, and an internal fusion peptide make up the S2 subunit. ACE2 is highly expressed in nasal epithelial cells, goblet/secretory cells, and ciliated cells, in addition to being found in many organs such as the heart, kidney, and gastrointestinal tract. Inside the host, the virus releases its subsequent genomic material, mRNA, in the cytoplasm and gets translated, thereby generating polyproteins, namely, pp1a and pp1b. These replicase polyproteins are further cleaved by virus-encoded proteinases into small proteins. Furthermore, ribosomal frameshifting occurs during the entire translation process, creating both genomic and multiple copies of subgenomic RNA species through discontinuous transcription encoding for important viral proteins. The viral RNA and protein interaction construct the virion, which is later discharged from the cells through the vesicles [12].

Membrane (M) protein of SARS-CoV-2

In the CoV particle, the M glycoprotein is the most abundant protein. It has 230 amino acids and three key parts—an N-terminal domain placed outside the virion membrane, three transmembrane domains, and a carboxy-terminal domain located inside the virus particle. In the virion, it occurs as a dimer with two conformations-long and compact (MLONG and MCOMPACT), which cause membrane curvature and nucleocapsid binding when coupled. M glycoprotein can enhance curvature before attaching to the nucleocapsid in a variety of ways. Furthermore, in alpha- and gamma-coronaviruses, N-linked glycosylation is common, whereas, in beta-coronaviruses, the common is O-linked glycosylation [13]. Reverse genetic studies have suggested that M glycoprotein promotes assembly by interacting with viral ribonucleoprotein and S glycoproteins at the budding site. It also forms a network of M-M interactions capable of preventing some host membrane proteins from interacting with the virus envelope. The protein plays a key role in virus assembly, where cellular membranes are transformed into workshops and the virus, together with host components, is gathered to produce new virus particles. M proteins interact through both the transmembrane domain and the endodomain. There is less evidence of detailed structure and functional information because of its tiny size, intimate interaction with the viral envelope, and tendency to form insoluble aggregate [14]. M protein's versatility is achieved through interactions with S, N, and E proteins. The interaction of S with M protein is required for the retention of S in the endoplasmic reticulum-Golgi intermediate compartment/Golgi complex and its integration into new virions. Furthermore, the interaction of M with N-protein stabilizes the N-protein and RNA complex, followed by the internal core of virions. In addition, the binding aids in the completion of viral assembly. Finally, the viral envelope is formed by the interaction of M with E protein, which is sufficient for both the synthesis and release of virus-like particles [15].

Envelope (E) protein of SARS-CoV-2

The envelope protein (E protein) is one of the smallest proteins compared to other proteins comprising 79–106 amino acids. Its size ranges from 8.4 to 12 kDa and consists of two structural domains: a large hydrophobic domain containing 25 amino acid residues and a hydrophilic carboxyl terminus that forms most of the protein [15]. The bizarre long hydrophobic stretch containing 25–30 amino acid residues is placed in between the hydrophilic N- and C-terminus [16]. The C-terminus is exposed to the cytoplasmic side, while the N-terminus is translocated across the membrane. An even-net charge distribution was discovered on both sides of the E-protein membrane. Only eight charged residues have been discovered in the protein sequence: two negatively charged residues preceding the transmembrane section, five charged residues, and one negatively charged residue in the C-terminal domain [17]. Interestingly during the replication cycle, only a few portions are assimilated into the virion envelope, and on the contrary, the protein is mostly expressed inside the infected cell [15]. Apart from the assembly of virions, E protein also plays an emerging role in virus entry, followed by the host stress response. The protein interacts with host proteins through ion channel activity leading to the

study of topologies of multiple membranes [18]. Moreover, depending on the genus of the virus, the need for E protein varies for the morphogenesis of the virus. The production of the virus is significantly compromised to approximately 1000-fold in the absence of envelope protein, thereby implementing that the protein plays an emerging role during morphogenesis [19]. The interaction between two proteins—E and M—is primarily essential for the budding process in pre-Golgi compartments, where the interlink of two proteins occurs because of cytoplasmic domains. The morphology of the Golgi apparatus is changed dramatically during the expression of E and thus explaining the importance of protein in inducing apoptosis. Incorporation into vesicles results because of the expression of protein alone, thereby promoting it to release from cells and the assembly of CoV-like particles is formed due to co-expression of the E protein with the other protein, namely, M, membrane protein [16].

Nucleocapsid protein of SARS-CoV-2

The CoV nucleocapsid protein is the most stable substructure of the viral particle composed of a thread-like strand, 8–9 mm in diameter, coiled or helical superstructure budding into the endoplasmic reticulum of infected cells. It is fairly flexible and almost shows the similarity of the structure with paramyxovirus nucleocapsids [20]. Aside from transcription and replication, the N protein is involved in the creation of helical ribonucleoproteins when the RNA genome is packed, as well as viral RNA synthesis regulation and infected cell metabolic modulation. Its architecture consists of three domains, namely, N-terminal RNA-binding domain (NTD) responsible for RNA binding, a C-terminal dimerization domain for oligomerization, and a central Ser/Arg (SR)-rich linker required for phosphorylation [21]. Moreover, being resolved by SDS-PAGE, the virion-associated-N protein of CoV was considered a single species of molecular weight ranging from 45–63 kDa depending upon the virus and strain. The protein is highly basic in that lysine and arginine amino acids predominate over aspartate and glutamate residues, accompanied by relatively high serine content (7–11%) [20]. The middle of the C-terminal region is essential for the antibodies to be elicited against SARS-CoV-2 during the immune response [22]. The primary characteristic that distinguishes N protein from other structural proteins is that it regulates the interlink of host and pathogen, such as reorganization of actin, progression of the host cell cycle, and apoptosis [21].

In silico molecular docking activity of active natural phytoconstituents against SARS-CoV-2

One of the well-known in silico methods for predicting the interlink between molecules and biological targets is molecular docking. This is accomplished by calculating a ligand's molecular familiarization with a receptor and then calculating its correlation using a docking score [23]. Different phytoconstituents demonstrated varying levels of binding effectiveness with SARS-CoV-2 targets. Interestingly, several phytoconstituents were found to have the ability to bind to numerous proteins. The literature review found that 100 phytoconstituents act on different targets of SARS-CoV-2. The list of the phytoconstituents is shown in Table 1. Table 2 enlists the binding probability of distinct classes of phytochemicals against different SARS-CoV-2 site proteins. Some of the phytoconstituents that show better stability with targets of SARS-CoV-2 based on their binding energy are shown in Table 3.

Binding affinity of phytoconstituents with Spike glycoprotein of SARS-CoV-2

The result achieved from the current review revealed that 23 was found to act on spike glycoprotein. Based on the available data reported in this review, the docking score of curcumin (− 115.198 kcal/mol) was found to be quite impressive followed by apigenin (− 108.614 kcal/mol), chrysophanol (− 107.385 kcal/mol), emodin (− 105.462 kcal/mol), zingerone (− 102.18 kcal/mol), gingerol (− 98.03 kcal/mol), and epigallocatechin gallate (− 91.72 kcal/mol) [24]. The chemical structure of some of the phytoconstituents inhibiting spike glycoprotein with superior binding energy is shown in Fig. 2. Contrary to our findings, the data reported in the literature revealed that some of the Food and Drug Administration (FDA)–approved drugs for SARS-CoV-2-like ivermectin, doxycycline, hydroxychloroquine, azithromycin, remdesivir, and oseltamivir also inhibited the spike glycoprotein with promising binding energies: − 102.63 kcal/mol, − 77.46 kcal/mol, − 69.19 kcal/mol, − 90.34 kcal/mol, − 83.36 kcal/mol, and − 81.45 kcal/mol, respectively [25]. This depicted that phytoconstituents may play an equal and significant role as FDA-approved drugs in the management of COVID-19 infections. Even though such compounds have shown potential binding efficacy as predicted by virtual in silico studies, there are still research gaps in which none of the phytoconstituents has been investigated for their efficacy against SARS-CoV-2. As a result, new preclinical and clinical initiatives are necessary to close this research gap.

Binding affinity of phytoconstituents with M.pro of SARS-CoV-2

Findings from the current review revealed that 77 phytoconstituents targeted the active sites of the M^{pro}. Some of the phytoconstituents with promising binding efficacy include laurolistine with a docking score of − 294.15 kcal/mol, acetoside (− 11.97 kcal/mol); cryptoquindoline (− 9.70 kcal/mol); avicularin (− 9.6 kcal/mol); cryptospirolepine (− 9.2 kcal/mol);

Table 1 In silico reports on the binding efficacy of various active phytoconstituents against SARS-CoV-2 protein/enzyme

Name of compound	Targeted protein/enzyme	Nature of interaction	Molecular interactions	Binding energy (kcal/mol) or docking score	Software utilized	References
Binding efficacy of phytoconstituents against M^{pro}						
10-Hydroxyusamberensine $C_{30}H_{28}N_4O$	M^{pro} PDB ID:6LU7	Inhibition	10-Hydroxyusamberesine forms a hydrogen link with the Gln-189 residue and a hydrophobic bond with the 6LU7 residues Tyr-54, Cys-145, Glu-166, Pro-168, and His-163	− 10.1	Autodock Vina 4.2	[27]
20-Epi-isoiguesterinol $C_{28}H_{38}O_3$	M^{pro} PDB ID:2DUC	Inhibition	20-Epi-isoiguesterinol forms hydrogen bonds with Thr-24, Thr-25 and interacts via hydrophobic bonds with Cys-145, His-41, and Met-165	− 9.3	Autodock Vina 4.2	[27]
22-Hydroxyhopan-3-one $C_{30}H_{50}O_2$	M^{pro} PDB ID:6LU7	Inhibition	While binding to 6LU7, 22-hydroxyhopan-3-one interacts with Lys-137 via a hydrogen bond and forms an alkyl and π -alkyl stacking with Leu-287, Leu-286, and Leu-275	− 8.70	Autodock Vina 4.2	[27]
3,5-Di-O-galloylshikimic acid $C_{21}H_{18}O_{13}$	M^{pro} PDB ID: 6LU7	Inhibition	Thr-190, His-163, and Asn-142 create hydrogen bonds with the hydroxyl group of the benzoyl moiety. Both benzoyl groups' hydroxyl and oxygen atoms create hydrogen bonds with Leu-167, Gly-143, and Glu-166	− 10.3	Schrodinger	[30]
6-Oxoisoguesterine $C_{30}H_{34}O_3$	M^{pro} PDB ID:6LU7	Inhibition	With Met-49, Met-165, and Cys-145 of 6LU7, 6-oxoisoguesterine forms a hydrogen bond with GLn-189 and forms an alkyl and π-alkyl stacking	− 9.10	Autodock Vina 4.2	[27]
Absinthin $C_{30}H_{40}O_6$	M^{pro} PDB ID:6LU7	Inhibition	Absinthin makes hydrogen bonds with His-163 and interacts via hydrophobic bond with Ser-144, Gly-143, Cys-145, Met-49, Met-165, Gln-189, Pro-168, Phe-140, Glu-166, Leu-141	− 8.2	Ligiplot + v.1.4.5	[32]
Acetoside $C_{29}H_{36}O_{15}$	M^{pro} PDB ID:6LU7	Inhibition	Acetoside formed hydrogen bonds with amino acid residues such as Thr-26, Phe-40, Glu-166, Leu-141, His-41, and Gln-189	− 11.97	Schrodinger suite v 12.3	[29]

Table 1 (continued)

Name of compound	Targeted protein/enzyme	Nature of interaction	Molecular interactions	Binding energy (kcal/mol) or docking score	Software utilized	References
Aiphanol $C_{25}H_{24}O_8$	M^{pro} PDB ID:6LU7	Inhibition	His-163, Ser-144, Leu-141, Cys-145, Gln-189, and Pro-168 form hydrogen bonds with aiphanol. When bound to the primary protease, it also undergoes hydrophobic interactions with His-172, His-163, Cys-145, His-141, Pro-168, Met-165, and Glu-166	−7.3	Autodock Vina	[41]
Anomalin $C_{24}H_{26}O_7$	M^{pro} PDB ID: 6Y84	Inhibition	His-41, Met-49, Cys-145, Met-165, and Pro-168 establish alkyl hydrophobic interactions with Anomalin, as well as π -alkyl and π -anion interactions with His-41 and Glu-166 of M^{pro}	−8.18	SwissDock	[42]
Astragalin $C_{21}H_{20}O_{11}$	M^{pro} PDB ID:6LU7	Inhibition	Astragalin forms hydrogen bonds with Leu-141 and Thr-190 and undergoes π- π stacking with His-163	−9.12	Schrodinger suite v 12.3	[29]
Avicularin $C_{20}H_{18}O_{11}$	M^{pro} PDB ID: 6LU7	Inhibition	With Cys-145 and Glu-166, Avicularin forms a hydrogen bond. It interacts hydrophobically with Hie-41. Furthermore, the hydroxyl group of the chromone nucleus and the benzene ring form hydrogen bonds with Thr-190, His-164, and Cys-145	−9.6	Schrodinger	[30]
Baicalin $C_{21}H_{18}O_{11}$	M^{pro} PDB ID:6LU7	Inhibition	Baicalin forms hydrogen bonds with Pro-168, Glu-166, Ser-144. It exhibits a C-H bond with Glu-166 and π-sulfur interaction with Cys-145 along with π-alkyl interaction with Met-49 of SARS-CoV-2 main protease	−8.1	Autodock Vina	[43]
Berberine $C_{20}H_{19}NO_5$	M^{pro} PDB ID:6LU7	Inhibition	Berberine forms hydrogen bond interaction with Phe-140, Asn-142 of 6LU7	−6.5	-	[44]

Table 1 (continued)

Name of compound	Targeted protein/enzyme	Nature of interaction	Molecular interactions	Binding energy (kcal/mol) or docking score	Software utilized	References
Calendoflaside $C_{28}H_{32}O_{15}$	M^{pro} PDB ID:6LU7	Inhibition	Calendoflaside interacted with 16 amino acid residues, 15 of which, Arg-188, Asp-187, Met-165, His-163, Ser-144, Glu-166, Phe-140, Leu-141, Cys-145, Gly-143, Asn-142, Leu-27, Met-49, Gln-189, His-41, are identical to those of native ligand, inhibitor N3 implying that Calendoflasid binds to a significant amino acid residue that inhibits the receptor protein M^{pro}	−8.5	Autodock Vina	[28]
Calendula glycoside-B $C_{48}H_{76}O_{19}$	M^{pro} PDB ID:6LU7	Inhibition	Calendula glycoside-B interacts with 16 amino acid residues among which 14 amino acids interaction, namely, Phe140, Ser144, His163, Glu166, Gln189, Arg188, Asp187, Leu141, His41, Met165, Gly143, Cys145, Asn142,His164 are similar to that of native ligand, inhibitor N3. Thus it can be inferred that calendula glycoside-B also interacts with major amino acid residues with which the native ligand interacts	−8.2	Autodock Vina	[28]
Calenduloside $C_{42}H_{68}O_{13}$	M^{pro} PDB ID:6LU7	Inhibition	Calenduloside interacts with 15 amino acid residues, 11 of which are identical to the native ligand N3, specifically Thr-25, Asn-142, Cys-145, His-164, Gln-189, Glu-166, Met-165, Gly-143, Leu-27, Thr-26, and Met-49	−7.9	Autodock Vina	[28]
Cardiofolioside B	M^{pro} PDB ID:6LU7	Inhibition	When cardiofoliside B binds to 6LU7, it forms hydrogen bonds with Ser-46, His-41, Cis-145, and Thr-24	−7.3	-	[44]

Table 1 (continued)

Name of compound	Targeted protein/enzyme	Nature of interaction	Molecular interactions	Binding energy (kcal/mol) or docking score	Software utilized	References
Carvacrol $C_{10}H_{14}O$	M^{pro} PDB ID:6LU7	Inhibition	When carvacrol binds to 6LU7, it creates three hydrogen interactions (-H) with His-41, Gln-189, and Thr-190	−4.82	Molecular Operating Environment	[45]
	M^{pro} PDB ID:2GTB	Inhibition	With 2GTB, only electrostatic interactions (Van der Waals) are perceptible; there are no non-perceptible interactions	−4.45		
Chebulagic` acid $C_{41}H_{30}O_{27}$	M^{pro} PDB ID:5R7Z	Inhibition	Chebulagic acid's carbonyl group creates a hydrogen bond with Gly-189. Chebulagic acid's ester creates a hydrogen bond with Ser-46 and Asn-142. Furthermore, the hydroxylic group on the phenyl ring can make hydrogen bonds with 5R7Z's Thr-26, Asn-142, and Glu-166	−7.641	Schrodinger (Maestro 11.4)	[46]
Cirsimaritin $C_{17}H_{14}O_6$	M^{pro} PDB ID:6LU7	Inhibition	When cirsimaritin binds to COVID-19's primary protease, it generates hydrogen bonds with residues Glu-166, His-163, Cys-145, Leu-141, and Ser-144	−7.2	AutoDock Vina	[33]
Corymbocoumarin $C_{21}H_{24}O_7$	M^{pro} PDB ID: 6Y84	Inhibition	Corymbocoumarin forms a C-H bond with Met-165, alkyl hydrophobic interaction with His-41, Cys-145, Met-49, Pro-168 and Met-165, π-anion interaction with Glu-166, π-lone pair interaction with Asn-142, π-alkyl interaction with His-41	−8.57	SwissDock	[42]
Cryptoquindoline $C_{31}H_{20}N_4$	M^{pro} PDB ID:6LU7	Inhibition	While binding to 6LU7, cryptoquindoline creates hydrophobic bonds with Met-298, Asp-294, Ala-113, Ser-114, and Thr-154	−9.70	Autodock Vina 4.2	[27]
Cryptospirolepine $C_{34}H_{24}N_4O$	M^{pro} PDB ID: 2DUC	Inhibition	Cryptoisoprenaline forms a hydrogen bond interaction with His-41 and interacts with Met-49, Glu-47, Glu-166, and Thr-25 of 2DUC via a hydrophobic bond	−9.20	Autodock Vina 4.2	[27]

Table 1 (continued)

Name of compound	Targeted protein/enzyme	Nature of interaction	Molecular interactions	Binding energy (kcal/mol) or docking score	Software utilized	References
Cyanidin3-glucoside $C_{21}H_{21}ClO_{11}$	M^{pro} PDB ID:6LU7	Inhibition	Cyanidin 3-glucoside creates hydrogen bond with Gln-189, Leu-141, Thr-26, Asp-187, and Glu-166 of the SARS-CoV-2 major protease, as well as carbon-hydrogen bonds with Gly-143 and π -alkyl interactions with Met-49 and Cys-145	−8.4	Autodock Vina	[43]
Dihydroergotamine $C_{33}H_{37}N_5O_5$	M^{pro} PDB ID: 2DUC	Inhibition	Dihydroergotamine forms two hydrogen bonds with Cys-143's backbone nitrogen and a hydrophobic bond with nine 2DUC amino acid residues: Thr-25, His-41, Cys-44, Met-49, Asn-142, Cys-145, His-164, Met-165, and Glu-166	−9.4	Autodock Tools-1.5.6	[48]
Dithymoquinone $C_{20}H_{24}O_4$	M^{pro} PDB ID:6LU7	Inhibition	While interacting with 6LU7, dithymoquinone makes only one hydrogen bond (H acceptor) with Thr-190	−4.45	Molecular Operating Environment	[45]
	M^{pro} PDB ID:2GTB	Inhibition	Non-perceptible interaction takes place with 2GTB, only electrostatic interactions (Van der Waals) are perceptible	−4.99		
Ergotamine $C_{33}H_{35}N_5O_5$	M^{pro} PDB ID: 6Y2F	Inhibition	While binding to 6Y2F, ergotamine generates hydrogen bonds with Gly-143 and interacts with Thr-25, His-41, Cys-44, Met-49, Asn-142, Cys-145, His-164, Met-165, Glu-166, Asp-187, Arg-188 via hydrophobic bonds	−9.3	Autodock Tools-1.5.6	[48]
Esculin $C_{15}H_{16}O_9$	M^{pro} PDB ID: 6Y84	Inhibition	Esculin forms hydrogen bonds with the amino acids Glu-166 and Gly-143, as well as a carbon-hydrogen bond with the amino acids Met-165 and Asn-142. M^{pro}'s His-41 and Cys-145 residues interact with esculin via carbon-hydrogen bonding and π sulfur interactions, respectively	−7.74	SwissDock	[42]

Table 1 (continued)

Name of compound	Targeted protein/enzyme	Nature of interaction	Molecular interactions	Binding energy (kcal/mol) or docking score	Software utilized	References
Glabridin $C_{20}H_{20}O_4$	M^{pro} PDB ID:6LU7	Inhibition	Glabridin interacts with Glu-166 electrostatically and hydrophobically with Met-49, Met-165, and His-41	−8.1	Autodock Vina	[43]
Gnetulcleistol $C_{26}H_{26}O_8$	M^{pro} PDB ID:6LU7	Inhibition	Gnetulcleistol forms hydrogen bonds with Thr-190, Gly-143, Leu-141, His-163 and Glu-166.It also forms a hydrophobic bond with residues, namely, Ala-191, Leu-50, Cys-145 and Leu-167	−7.3	Autodock Vina	[41]
Heraclenol $C_{16}H_{16}O_6$	M^{pro} PDB ID: 6Y84	Inhibition	Heraclenol establishes hydrogen bonds with His-41, Ser-144, Asn-142, Cys-145, Met-145, and Met-49, as well as C-H bonds and π -alkyl interactions with Cys-145, Met-145, and Met-49. It also forms a π-donor hydrogen bond with M^{pro}'s Glu-166	−8.20	SwissDock	[42]
Hispidulin $C_{16}H_{12}O_6$	M^{pro} PDB ID:6LU7	Inhibition	By binding with COVID-19's primary protease, Hispidulin creates hydrogen bonds with amino acids such as His-163, Leu-141, Ser-144, Glu-166, and Cys-145	−7.3	AutoDock Vina	[33]
Hypericin $C_{30}H_{16}O_8$	M^{pro} PDB ID:6LU7	Inhibition	Hypericin makes hydrogen bonds with Glu-166, Leu-141, Asn-142, Glu-166 (pi-sigma), Gln-189 (pi-sigma), Met-165 (pi-alkyl), and Cys-145 (pi-alkyl) of SARS-CoV-2 major protease	−10.7	Autodock Vina	[43]
Isofraxidin $C_{11}H_{10}O_5$	M^{pro} PDB ID: 6Y84	Inhibition	Isofraxidin establishes hydrogen bonds with His-164, Met-165, Gln-189, and Glu-166, and has a π -alkyl interaction with Met-165, a C-H bond with Gln-189, and a π -donor hydrogen link with Glu-166	−7.00	SwissDock	[42]
Isorhamnetin-3-O-β-D $C_{22}H_{22}O_{12}$	M^{pro} PDB ID:6LU7	Inhibition	Isorhamnetin-3-O-β-D interacted with 16 amino acid residues, with 13 of them matching the inhibitor N3, specifically Cys-145, Gly-143, Asn-142, Ser-144, His-163, Phe-140, Gln-189, Asp-187, Arg-188, Met-165, His-41, Thr-26, Met-49	−8.7	Autodock Vina	[28]

Table 1 (continued)

Name of compound	Targeted protein/enzyme	Nature of interaction	Molecular interactions	Binding energy (kcal/mol) or docking score	Software utilized	References
Kellerin $C_{26}H_{34}O_6$	M^{pro} PDB ID: 6Y84	Inhibition	With Asn-142 and Met-165, Kellerin forms C-H bonds, alkyl hydrophobic contacts with His-41 and Cys-145, and π -alkyl interactions with Cys-145	−8.18	SwissDock	[42]
Laurolistine $C_{18}H_{19}NO_4$	M^{pro} PDB ID: 5RE4	Inhibition	Laurolistine interacts with amino acid residues Glu-166 and Asn-142 via hydrogen bonding	−294.15	Discovery Studio	[26]
Luteoline $C_5H_{10}O_6$	M^{pro} PDB ID:5R7Y	Inhibition	The OH group of luteoline forms four hydrogen bonds with Asn- 142, Hie-41, Gln-192, Thr-190 of 5R7Y	−7.129	Schrodinger (Maestro 11.4)	[46]
Maackolin $C_{25}H_{23}O_8$	M^{pro} PDB ID: 6LU7	Inhibition	Thr-190, Arg-188, Glu-166, Asn-142, Gly-143, Cys-145, Ser-144, His-163 and Glu-166 create hydrogen bonds with Maackolin. When it binds to the main protease, it generates hydrophobic interactions with Met-165, His-163, His-172, Cys-145, and Phe-140	−8.2	Autodock Vina	[41]
Mesuol $C_{24}H_{24}O_5$	M^{pro} PDB ID: 6Y84	Inhibition	Through π-alkyl interaction, Mesuol interacts with His-41, Cys-44, and Met-49. Between mesuol and Glu-166, a hydrogen bond is formed, followed by a Vander Waals contact with Cys-145	−7.38	SwissDock	[42]
Methylgalbanate $C_{25}H_{32}O_5$	M^{pro} PDB ID: 6Y84	Inhibition	Methylgalbanate creates hydrophobic interactions with Cys-145, His-41, His-163, Met-165, Leu-167, -alkyl interactions with Cys-145, C-H bond with Asn-142, Glu-166, and π -alkyl interactions with Cys-145, His-41, His-163, Met-165, Leu-167	−8.30	SwissDock	[42]
Narcissin $C_{28}H_{32}O_{16}$	M^{pro} PDB ID:6LU7	Inhibition	Narcissin interacted with 13 amino acid residues, 11 of which are identical to the native ligand N3, namely, Leu-141, Asn-142, Cys-145, Gly-143, Leu-27, Met-49, Asp-187, Met-165, His-41, Gln-189, and Arg-188	−8.4	Autodock Vina	[28]

Table 1 (continued)

Name of compound	Targeted protein/enzyme	Nature of interaction	Molecular interactions	Binding energy (kcal/mol) or docking score	Software utilized	References
Nigellicine $C_{13}H_{14}N_2O_3$	M^{pro} PDB ID:6LU7	Inhibition	While interacting with 6LU7, Nigellicine creates hydrogen bonds with Thr-190 and Glu-166	−5.11	Molecular Operating	[45]
	M^{pro} PDB ID:2GTB	Inhibition	When Nigellicine interacts with 2GTB, it creates hydrogen bonds with Cys-145(H-donor), Gly-143, and Cys-145(H-acceptor)	−5.05	Environment	
Nigellidine $C_{18}H_{18}N_2O_2$	M^{pro} PDB ID:6LU7	Inhibition	Upon interacting with 6LU7, nigellidine forms two possible hydrogen interactions with Met-49 and Thr-190	−6.29	Molecular Operating Environment	[45]
	M^{pro} PDB ID:2GTB	Inhibition	Nigellidine forms only one hydrogen bond with His-163 while interacting with 2GTB	−5.58		
Nigellimine $C_{12}H_{13}NO_3$	M^{pro} PDB ID:6LU7	Inhibition	No possible interaction with 6LU7 takes place only Vander Waals exist	−4.80	Molecular Operating	[45]
	M^{pro} PDB ID:2GTB	Inhibition	While binding to 2GTB, Nigellimine creates only one hydrogen interaction (π-π) with His-141	−5.07	Environment	
Osthole $C_{15}H_{16}O_3$	M^{pro} PDB ID: 6Y84	Inhibition	Osthole forms only one hydrogen bond with Gly-143.It also exhibits hydrophobic interactions with Cys-145 and His-163 and π-alkyl interactions with Cys-145 and Met-49	−7.24	SwissDock	[42]
Oxypeucedanin $C_{16}H_{14}O_5$	M^{pro} PDB ID: 6Y84	Inhibition	Gly-143 forms a hydrogen bond with Oxypeucedanin, as well as C-H bonds with His-41, Cys-44, and Asn-142, alkyl hydrophobic interactions with Cys-145, His-41, and Leu-27, and π -alkyl interactions with Met-49 of M^{pro}	−7.26	SwissDock	[42]
Pabulenol $C_{16}H_{14}O_5$	M^{pro} PDB ID: 6Y84	Inhibition	Pabulenol forms hydrogen bonds with Leu-141, Cys-145, His-163, Met-49, and Asn-142, as well as π-sulfur interactions with Cys-145, π-alkyl interactions with His-163, Met-49, and C-H bonds with Asn-142	−7.42	SwissDock	[42]

Table 1 (continued)

Name of compound	Targeted protein/enzyme	Nature of interaction	Molecular interactions	Binding energy (kcal/mol) or docking score	Software utilized	References
Pranferol $C_{16}H_{16}O_5$	M^{pro} PDB ID: 6Y84	Inhibition	Pranferol creates hydrogen bonds with Glu-166, π-alkyl interactions with Pro-168 and Met-165, alkyl hydrophobic interactions with Pro-168, C-H bonds with Thr-190 and Gln-189, and alkyl hydrophobic interactions with Pro-168	−7.16	SwissDock	[42]
Procyanidin-A3 $C_{75}H_{62}O_{30}$	M^{pro} PDB ID:6LU7	Inhibition	When Procyanidin-A3 binds to the active site of the major protease, it creates hydrogen bonds with amino acid residues Pro-168, Glu-166, Thr-190, and Gln-189	−12.86	Schrodinger suite v 12.3	[29]
Rhein $C_{15}H_8O_6$	M^{pro} PDB ID:6LU7	Inhibition	The amino acid residues, namely, Lys-102, Val-104, Ile-106, Gln-110, Thr-29, Thr-111, Phe-294, Asp-295, Gln-127, Phe-8, Asn-151, Ile-152, Asp-153 and Ser-158 participated in the interaction of Rhein at the binding pocket of 6LU7	−8.1	Autodock Tool	[51]
Rutamarin $C_{21}H_{24}O_5$	M^{pro} PDB ID: 6Y84	Inhibition	Rutamarin forms a hydrogen bond with Ser-46 and Glu-166, alkyl hydrophobic interactions with His-41, Met-165 and Met-49, π-alkyl interaction with Cys-145, His-41, C-H bond formation with Thr-45	−7.63	SwissDock	[42]
Rutin $C_{27}H_{30}O_{16}$	M^{pro} PDB ID:6LU7	Inhibition	Rutin interacts with sixteen amino acid residues out of which fifteen residues, namely, Ser-144, His-163. Asn-142, Cys-145, Gly-143, His-41, Phe-140, Thr-25, Thr-26, Thr-190, Arg-188, Met-165, Glu-166, His-164, Leu-141, Gln-189 matches with that to the inhibitor N3. Thus it can be predicted that rutin binds to the entire amino acid residue needed for the proper inhibition of receptor protein, M^{pro}	−8.8	Autodock Vina	[28]

Table 1 (continued)

Name of compound	Targeted protein/enzyme	Nature of interaction	Molecular interactions	Binding energy (kcal/mol) or docking score	Software utilized	References
Saxalin $C_{16}H_{15}ClO_5$	M^{pro} PDB ID: 6Y84	Inhibition	Saxalin forms C-H bond with Leu-141, His-41, π-donor hydrogen bond with Glu-166, π-sigma interaction with His-41, alkyl hydrophobic interaction with His-41 and Met-49, π-alkyl interaction with Met-165, π-sulfur interaction with Cys-145 of M^{pro}	−7.14	SwissDock	[42]
Scutallarin $C_{15}H_{10}O_6$	M^{pro} PDB ID:5R82	Inhibition	The hydroxyl group of Scutellarein forms a hydrogen bond with amino acids Thr-26, Gly-189. The 4-oxo chromene group also forms hydrogen bonding interaction with Gly-143 and (π- π) stacking interaction takes place between phenyl ring and Hie-41 of 5R82	−7.031	Schrodinger (Maestro 11.4)	[46]
Scutellarein 7-glucoside $C_{21}H_{20}O_{11}$	M^{pro} PDB ID: 6LU7	Inhibition	Scutellarein 7-glucoside forms a hydrogen bond with Cys-145, His-163, Glu-166 due to the hydroxyl group of the sugar moiety. Moreover, the hydroxyl group of phenyl rings also interacts with Gln-192 through hydrogen bonding	−9.3	Schrodinger	[30]
Scutellarein 7-glucoside $C_{21}H_{20}O_{11}$	M^{pro} PDB ID:4MDS	Inhibition	While interacting with the main protease, the hydroxyl group of the sugar moiety makes hydrogen bonds with His-41, Thr-190, Ala-191, Glu-166, Asn-142, Asn-119, Thr-26, and Thr-24	−7.43	Schrodinger	[30]
Seselin $C_{14}H_{12}O_3$	M^{pro} PDB ID: 6Y84	Inhibition	Seselin forms a hydrogen bond with Gly-143, π-alkyl interaction with Cys-145, His41 and Met-165, alkyl hydrophobic interaction with Cys-145 and Leu-27	−7.00	SwissDock	[42]
Solanine $C_{45}H_{73}NO_{15}$	M^{pro} PDB ID:6LU7	Inhibition	Solanine forms a hydrogen bond with Glu-166, His-164, Leu-141 and Gln-189 upon binding with the active site of the main protease	−10.30	Schrodinger suite v 12.3	[29]

Table 1 (continued)

Name of compound	Targeted protein/enzyme	Nature of interaction	Molecular interactions	Binding energy (kcal/mol) or docking score	Software utilized	References
Sphondin $C_{12}H_8O_4$	M^{pro} PDB ID: 6Y84	Inhibition	Sphondin forms a C-H bond with His-163, Leu-141, Asn-142, π-alkyl interaction with Cys-145, Met-165 and Met-49	−6.94	SwissDock	[42]
Tembetarine $C_{20}H_{26}NO_4+$	M^{pro} PDB ID:6LU7	Inhibition	Tembetarine undergoes hydrogen bond interaction with Glu-166, His-163 while binding 6LU7	−6.6	-	[44]
Thymohydroquinone $C_{10}H_{14}O_2$	M^{pro} PDB ID:6LU7	Inhibition	Thymohydroquinone forms only one hydrogen interaction (π-H) with Glu-166 while binding 6LU7	−4.22	Molecular Operating Environment	[45]
	M^{pro} PDB ID:2GTB	Inhibition	Thymohydroquinone forms only one hydrogen bond with Gly-143 while binding 2GTB	−4.23		
Thymol $C_{10}H_{14}O$	M^{pro} PDB ID:6LU7	Inhibition	Thymol forms only one hydrogen interaction(π-H) with Gln-189 while binding with 6LU7	−4.50	Molecular Operating Environment	[45]
	M^{pro} PDB ID:2GTB	Inhibition	Thymol on binding with 2GTB forms only electrostatic interactions (Van der Waals)	−4.03		
Thymoquinone $C_{10}H_{12}O_2$	M^{pro} PDB ID:6LU7	Inhibition	Thymoquinone forms only one hydrogen interaction (π-H) with Thr-190 while binding with 6LU7	−4.71	Molecular Operating Environment	[45]
	M^{pro} PDB ID:2GTB	Inhibition	There are non-perceptible interaction with 2GTB,only electrostatic interactions (Van der Waals) are perceptible	−4.41		
Tinosponone $C_{19}H_{22}O_5$	M^{pro} PDB ID:6LU7	Inhibition	Tinosponone forms hydrogen bond interaction with Glu-166, Asn-142 while binding 6LU7	−7.7	-	[44]
Vasicinone $C_{11}H_{10}N_2O_2$	M^{pro} PDB ID:5R7Z	Inhibition	Hydroxyl group of Vasicinone forms hydrogen bond with Glu-166 and (π- π) stacking interaction takes place between phenyl ring and Hie-41 while binding 5R7Z	−7.49	Schrodinger (Maestro 11.4)	[46]

Table 1 (continued)

Name of compound	Targeted protein/enzyme	Nature of interaction	Molecular interactions	Binding energy (kcal/mol) or docking score	Software utilized	References
Withaferin-A $C_{28}H_{38}O_6$	M^{pro} PDB ID:6LU7	Inhibition	The amino acid residues, namely, Phe-294, Thr-292, Asp-295, Asp-153, Ser-158, Lys-102, Phe-103, Glu-178, Arg-105, Ile-106, Gln-110, Thr-111, Gln-178 and Val-108 participated in the interaction of Withaferin-A at the binding pocket of 6LU7	−7.7	Autodock Tool	[51]
Withanolide-D $C_{28}H_{38}O_6$	M^{pro} PDB ID:6LU7	Inhibition	Lys-102, Phe-103, Val-104, Arg-105, Ile-106, Gln-107, Gln-110, Phe-294, Phe-8, Asn-151, Tyr-154 and Asp-153 participated in the interaction of Withanolide-D at the binding pocket of 6LU7	−7.8	Autodock Tool	[51]
Xanosporic acid $C_{28}H_{24}O_{11}$	M^{pro} PDB ID:6LU7	Inhibition	Xanosporic acid forms hydrogen bond interaction with His-41, His-163, Gln-189 while binding 6LU7	−7.5	-	[44]
Xanthotoxin $C_{12}H_8O_4$	M^{pro} PDB ID: 6Y84	Inhibition	Xanthotoxin forms a hydrogen bond with Gly-143 and Glu-166, π-sulfur interaction with Cys-145 and π-alkyl interaction with Met-165, C-H bond with Glu-166 of M^{pro}	−6.80	SwissDock	[42]
α-hederin $C_{41}H_{66}O_{12}$	M^{pro} PDB ID:6LU7	Inhibition	While interacting with the primary protease, α-hederin generates three hydrogen bonds with His-165 (H donor), Cys-145, and Met-165	−5.25	Molecular Operating Environment	[45]
	M^{pro} PDB ID:2GTB	Inhibition	α-Hederin in complex with 2GTB forms only one hydrogen bond with Gly-143 (H acceptor)	−6.50		
α-ketomide-11r $C_{33}H_{40}N_4O_5$	M^{pro} PDB ID:6LU7	Inhibition	Asn-142, Gly-143, Ser-144, Cys-145, Phe-140, and His-164 create hydrogen bonds with α-ketomide-11r. It also has a hydrophobic interaction with the SARS-CoV-2 major protease's His-41 and Met-49	−7.8	Autodock Vina	[43]

Table 1 (continued)

Name of compound	Targeted protein/enzyme	Nature of interaction	Molecular interactions	Binding energy (kcal/mol) or docking score	Software utilized	References
Binding efficacy of phytoconstituents against ACE-2						
3,5-Di-O-galloylshikimic acid $C_{21}H_{18}O_{13}$	ACE-2 PDB ID:1R4L	Inhibition	Through non-covalent ionic contact, the oxygen of carboxylate in 3,5-Di-O-galloylshikimic acid forms hydrogen bonds with Hie-505, Hie-345, and Arg-273 in ACE2. The benzoyl moiety's hydroxyl group creates hydrogen bonds with Tyr-127 and Glu-406. One of the benzoyl rings was involved in π- π stacking interaction with Hie-345 of the side chain	− 11.2	Schrodinger	[30]
Absinthin $C_{30}H_{40}O_6$	ACE-2 PDB ID:1R4L	Inhibition	Absinthin forms hydrogen bonds with Thr-371, Thr-445, and Asp-269, as well as hydrophobic bonds with Trp-271, Pro-346, Phe-274, Arg-518, Asp-367, Thr-276, Asn-277, Ala-153, and Asn-149	− 11.8	Ligiplot + v.1.4.5	[32]
Avicularin $C_{20}H_{18}O_{11}$	ACE-2 PDB ID:1R4L	Inhibition	Avicularin forms π-cation interaction with Arg-273, whereas the main nucleus' carbonyl group, interacts with Arg-518 via hydrogen bonding	-8.0	Schrodinger	[30]
Cirsimaritin $C_{17}H_{14}O_6$	ACE-2 PDB ID:1R42	Inhibition	Crismaritin forms hydrogen bonds with amino acids residue, namely, Tyr-196 and Asp-206 while binding with ACE2	-7.6	AutoDock Vina	[33]
Hispidulin $C_{16}H_{12}O_6$	ACE-2 PDB ID:1R42	Inhibition	While binding with ACE2, hispidulin produces hydrogen bonds with the amino acids Tyr-196, Gly-564, and Trp-566	-7.8	AutoDock Vina	[33]
Scutellarein 7-glucoside $C_{21}H_{20}O_{11}$	ACE-2 PDB ID:1R4L	Inhibition	The hydroxyl group of sugar moiety interacts with Glu-375, Hie-345 and Hie-505 through the formation of a hydrogen bond. The phenyl ring makes π- π stacking interaction with Hie-345. The carbonyl oxygen and the hydroxyl group of the chromone nucleus forms a hydrogen bond with Thr-371 and Ash-368	− 10.6	Schrodinger	[30]

Table 1 (continued)

Name of compound	Targeted protein/enzyme	Nature of interaction	Molecular interactions	Binding energy (kcal/mol) or docking score	Software utilized	References
Binding efficacy of phytoconstituents against PL^{pro}						
Asparoside-C $C_{57}H_{96}O_{27}$	PL^{pro} PDB ID:6WX4	Inhibition	The positively charged Lys-157, Arg-166, polar Thr-301, negatively charged Glu-161, Asp-164, Glu-167, and hydrophobic Pro-248 create hydrogen bonds with hydroxyl group of asparoside-C	−5.44	Schrodinger	[35]
Binding efficacy of phytoconstituents against RdRp						
Asparoside-C $C_{57}H_{96}O_{27}$	RdRp PBD ID:6MJ1	Inhibition	Asparoside-C's glycone occupies the binding site in such a way that the molecule's primary glycosidic component fits into a binding cavity surrounded by hydrophobic Tyr-455, Tyr-458, and Val-166 residues. Lys-798, Glu-167, Tyr-455, Arg-457, Asn-691, Asp-623, Asp-452, Lys-798, Glu-167, Tyr-455, Arg-457, Asn-691, Asp-623, Asp-452, Lys-798, Glu-167, Tyr-455, Arg-457, Asn-691, Asp-623, Asp-452. While interacting with RNA dependent RNA polymerase, the oxygen atom from the glycosidic linkage creates a hydrogen bond with Lys-621 residue	-6.65	Schrodinger	[35]
Binding efficacy of phytoconstituents against S-RBD						
Asparoside-C $C_{57}H_{96}O_{27}$	S-RBD PDB ID:6M0J	Inhibition	Asparoside-C's hydroxyl group forms hydrogen bonds with Gly-496, Gln-414, and Ser-494, whereas the hydroxyl group of the other oxane ring forms bi-furcated hydrogen bonds with hydrophilic acceptor Ser-494 and hydrophobic donor Tyr-453. While binding to the SARS –CoV-2 spike receptor-binding domain, the hydroxyl group of terminal oxane interacted with Gln-414, Thr-415, and the hydroxymethyl group of terminal oxane ring displayed hydrogen bonding with Gln-414	−7.16	Schrodinger	[35]

Table 1 (continued)

Name of compound	Targeted protein/enzyme	Nature of interaction	Molecular interactions	Binding energy (kcal/mol) or docking score	Software utilized	References
Asparoside-D $C_{56}H_{94}O_{27}$	S-RBD PDB ID:6M0J	Inhibition	While interacting with the SARS-CoV-2 spike receptor-binding domain, the hydroxyl group of Asparoside-D establishes hydrogen bonds with residues such as Gly-502, Ser-494, Lys-417, and Asp-420, whereas the hydroxyl group of another oxane ring showed bi-furcated hydrogen bonding with Tyr-449 and Gln-498	−7.06	Schrodinger	[35]
Shatavarin-I $C_{51}H_{86}O_{23}$	S-RBD PDB ID:6M0J	Inhibition	Hydroxyl group of oxane ring of Shatavarin-I exhibits bifurcated hydrogen bonding with residues, namely, Glu-406 and Gly-496 while interacting with SARS -CoV-2 spike receptor-binding domain	−6.52	Schrodinger	[35]
Binding efficacy of phytoconstituents against SARS-CoV-2 E						
Belachinal $C_{30}H_{46}O_5$	SARS-COV-2 E PDB ID: 5X29	Inhibition	Belachinal forms hydrophobic bond with Ala-22, Leu-19, Val-29, Val-25, Phe-23, Phe-26, Leu-19	−11.46	Discovery studio	[36]
Macaflavanone E -	SARS-CoV-2 E PDB ID:HG1	Inhibition	While binding HG1, mecaflavanone E creates hydrophobic bonds with Phe-23, Val-25, Leu-27, Val-24, Leu-65, Phe-26, and Ala-22	−11.07	Discovery Studio	[36]
Vibsanol B $C_{25}H_{36}O_6$	SARS-CoV-2 E PDB ID:HG1	Inhibition	Vibsanol B forms a hydrophobic bond with Thr-30, Ala-22, Val-25, Val-29, Phe-23, Phe-26, Ile-33	−11.07	Discovery Studio	[36]
Binding efficacy of phytoconstituents against NSP15 Endoribonuclease						
Asparoside-C $C_{57}H_{96}O_{27}$	NSP15 endoribonuclease PDB ID:6W01	Inhibition	While interacting NSP15 endoribonuclease, the hydroxyl group of the oxane ring of Asparoside-C was stabilized by hydrogen bonding with Glu-234, Gly-230, Val-292, Hip-235, Asp-240, while the hydroxymethyl group displayed hydrogen bonding with Val-292	−7.54	Schrodinger	[35]

Table 1 (continued)

Name of compound	Targeted protein/enzyme	Nature of interaction	Molecular interactions	Binding energy (kcal/mol) or docking score	Software utilized	References
Asparoside-D $C_{56}H_{94}O_{27}$	NSP15 endoribonuclease PDB ID:6W01	Inhibition	The hydroxyl group of Asparoside-D forms hydrogen bonds with residues such as Glu-340, His-243, Gln-245, Asp-240, and the terminal hydroxymethyl group forms bi-furcated hydrogen bonds with Asn-278 and Leu-346	−6.44	Schrodinger	[35]
Saikosaponin C $C_{48}H_{78}O_{17}$	NSP15 endoribonuclease PDB ID:6W01	Inhibition	Saikosaponin C forms a hydrogen bond with residues, namely, Lys-290, Gln-245, hip-235, Thr-341, Asn-278 and Leu-346 while binding with SARS-CoV-2 NSP15 endoribonuclease. It also interacts via hydrophobic bond with residues, namely, Val-292, Leu-346, Pro-344, Tyr-343, Trp-333, Cys-293, Leu-246, Gly-247 and Gly-248 of SARS-CoV-2 NSP15 endoribonuclease	−6.98	Schrodinger maestro	[38]
Saikosaponin K $C_{54}H_{88}O_{22}$	NSP15 endoribonuclease PDB ID:6W01	Inhibition	Saikosaponin K forms a hydrogen bond with amino acid residues, namely, Val-292, Hip-250, Gly-248, Tyr-343 and Glu-340 while binding with SARS-CoV-2 NSP15 endoribonuclease. Moreover, it also exhibits a hydrophobic bond with Val-292, Leu-246, Tyr-343, Trp-333, Cys-293, Gly-247, Gly-248, Cys-291, Met-331 and Ala-232	−6.79	Schrodinger maestro	[38]
Saikosaponin U $C_{59}H_{96}O_{29}$	NSP15 endoribonuclease PDB ID:6W01	Inhibition	Saikosaponin U forms a hydrogen bond with Asp-240, Hip-250, Lys-290, Hip-235, Thr-341, Glu-234, Tyr-343 and Glu-340 while binding with SARS-CoV-2 NSP15 endoribonuclease. It also interacts via hydrophobic bond with residues, namely, Val-339, Leu-246, Pro-344, Tyr-343, Trp-333, Val-292, Cys-293 and Ala-232 of SARS-CoV-2 NSP15 endoribonuclease	-7.27	Schrodinger maestro	[38]

Table 1 (continued)

Name of compound	Targeted protein/enzyme	Nature of interaction	Molecular interactions	Binding energy (kcal/mol) or docking score	Software utilized	References
Saikosaponin V $C_{53}H_{86}O_{24}$	NSP15 endoribonuclease PDB ID:6W01	Inhibition	Saikosaponin V forms a hydrogen bond with amino acid residues, namely, Glu-234, Asn-278, Pro-344, Val-292, Tyr-343, Leu-346, Glu-340 and Gln-245. It also interacts via hydrophobic bond with Trp-333, Pro-344, Gly-230, Leu-346, Tyr-343, Val-339, Ala-232, Cys-291 and Val-292 while binding with SARS-CoV-2 NSP15 endoribonuclease	− 8.35	Schrodinger maestro	[38]
Binding efficacy of phytoconstituents against spike protein						
Ajoene $C_9H_{14}OS_3$	Spike protein PDB ID:6VYB	Inhibition	When ajoene binds to the SARS-CoV-2 spike protein, it establishes two hydrogen bonds with Gln-1010 and Thr-1009	− 74.2819	iGEMDOCK	[24]
Apigenin $C_{15}H_{10}O_5$	Spike protein PDB ID:6VYB	Inhibition	While binding to SARS-CoV-2 Spike protein, curcumin forms hydrogen bonds with Asn-544, Arg-567, Asn-978, Asp-979, Ala-522, and Thr-547	− 108.614	iGEMDOCK	[24]
Chrysophanol $C_{15}H_{10}O_4$	Spike protein PDB ID:6VYB	Inhibition	Chrysophanol interacts with the SARS-CoV-2 spike protein by forming hydrogen bonds with the amino acid residues like Asp-1041, Gly-1044, and Gly-1046	− 107.385	iGEMDOCK	[24]
Cinnamtannin-B1 $C_{45}H_{36}O_{18}$	Spike Protein PDB ID:6LZG	Inhibition	Cinnamtannin-B1 forms hydrogen bonds with Phe-A:390, Asn-A:394 and Arg-A:393. It also exhibits hydrophobic interaction with Phe-A:40, Trp-A:349, Thr-A:347	− 10.2	Autodock Tool	[47]
Curcumin $C_{21}H_{20}O_6$	Spike protein PDB ID:6VYB	Inhibition	Curcumin creates hydrogen bonds with Asn-544, Arg-567, Asn-978, Asp-979, Ala-522, and Thr-547 when it binds to spike protein	− 115.198	iGEMDOCK	[24]
Emodin $C_{15}H_{10}O_5$	Spike protein PDB ID:6VYB	Inhibition	When Emodin binds to SARS-CoV-2 spike protein, it forms hydrogen bonds with Lys-1038, Gly-908, and His-1048	− 105.462	iGEMDOCK	[24]

Table 1 (continued)

Name of compound	Targeted protein/enzyme	Nature of interaction	Molecular interactions	Binding energy (kcal/mol) or docking score	Software utilized	References
Epigallocatechin gallate $C_{22}H_{18}O_{11}$	Spike protein PDB ID:6VYE	Inhibition	Gln-314, Asn-317, Asp-737, Asn-764, Thr-859, Thr-315, Val-736, and Asp-737 of the SARS-CoV-2 Spike protein interact with Epigallocatechin gallate through hydrogen bonding	−91.72	Autodock	[24]
Epitheaflavin monogallate $C_{36}H_{28}O_{16}$	Spike protein PDB ID:6M0J	Inhibition	Gly-496 and Glu-406 create hydrogen bonds with Epitheaflavin monogallate. Furthermore, when spike glycoprotein was bound, it revealed π- π interaction with Tyr-449	−7.52	Schrodinger suite v 12.3	[29]
Fisetin $C_{15}H_9O_6$	Spike protein PDB ID: 6VYB	Inhibition	Fisetin forms hydrogen bonds with Ser-730, Thr-778, and His-1058, as well as hydrophobic interactions with Ile-870, Pro-880, and Thr-732 residues of the spike protein's S2 domain	−8.5	Autodock Vina	[49]
Gingerol $C_{17}H_{26}O_4$	Spike protein PDB ID:6VYB	Inhibition	While binding with SARS-CoV-2 spike protein, gingerol generates hydrogen bonds with His-1058, Ala-1056, and Gly-1059	−98.03	iGEMDOCK	[24]
Luteline-7-glucoside-3'-glucoronide $C_{27}H_{28}O_{18}$	Spike protein PDB ID:6LZG	Inhibition	Tyr A:196, Glu A:564, Lys A:562, Gly A:395, Asn A:397, Arg A:514 and Glu A:398 create hydrogen bonds with Luteline-7-glucoside-3'-glucoronide. Tyr A:202 and Gly A:205 are two amino acid residues with which it forms two hydrophobic interactions	−10.1	Autodock Vina	[50]
Melitric acid A $C_{27}H_{20}O_{11}$	Spike protein PDB ID:6LU7	Inhibition	While interacting with the primary protease, melitric acid A creates three hydrogen bonds with amino acid residues, notably Gln A:110, Asn A:151, and Ile A:249, and five hydrophobic interactions with Val A:104, Ile A:106, Phe A:294, Pro A:293 and Ile A:249	−8.2	Autodock Vina	[50]

Table 1 (continued)

Name of compound	Targeted protein/enzyme	Nature of interaction	Molecular interactions	Binding energy (kcal/mol) or docking score	Software utilized	References
	Spike protein PDB ID:6LZG	Inhibition	While binding with spike protein, melitric acid A generates hydrogen bonds with residues like Tyr A:196, Lys A:562, Asn A:210, Glu A:564, Ser A:511, and Glu A:398. It also forms three hydrophobic connections with amino acid residues (Leu A:95, Val A:209, and Pro A:555), as well as one electrostatic interaction with Asp A:206	−10		
Pavetannin-C1 $C_{60}H_{48}O_{24}$	Spike Protein PDB ID:6LZG	Inhibition	Procyanidin-B7 establishes hydrogen bonds with Arg-A:131, Lys-A:137, Thr-A:199, and Leu-A:287, and solely interacts with Leu-A:286 and Glu-A:290 via hydrophobic and electrostatic interactions	−8.2	Autodock Tool	[47]
Procyanidin-B7 $C_{30}H_{26}O_{12}$	Spike Protein PDB ID:6LZG	Inhibition	Asp-A:206 and Asn-A:210 create hydrogen bonds with procyanidin-B7. It interacts hydrophobically with Leu-A:95, Val-A:209, and Pro-A:565 as well as electrostatically with Asp-A:206, Lys-A:562, Glu-A:402, and Asp-A:382	−9.6	Autodock Tool	[47]
Quadranoside III $C_{36}H_{58}O_{11}$	Spike protein PDB ID:6LZG	Inhibition	When interacting with spike protein, quadranoside III creates just two hydrogen bonds with Leu A:391 and Asn A:394 and two hydrophobic contacts with Phe A:40 and His A:401	−9.2	Autodock Vina	[50]
Quercitrin $C_{21}H_{20}O_{11}$	Spike protein PDB ID:6M0J	Inhibition	Quercitrin forms a hydrogen bond with Glu-406, Gly-496 and Ser-494. It also forms π-cation and π- π stacking with Arg-403 and Tyr-505 while binding with spike glycoprotein	−7.15	Schrodinger suite v 12.3	[29]

Table 1 (continued)

Name of compound	Targeted protein/enzyme	Nature of interaction	Molecular interactions	Binding energy (kcal/mol) or docking score	Software utilized	References
Saikosaponin C $C_{48}H_{78}O_{17}$	Spike protein PDB ID:6VSB	Inhibition	Saikosaponin C forms a hydrogen bond with residues, namely, Phe-403, Asp-345, Lys-341 and Glu-372 while binding with SARS-CoV-2 spike glycoprotein. It also forms a hydrophobic bond with residues, namely, Val-299, Tyr-313, Tyr-338, Leu-342, Pro-343, Phe-346, Pro-370, Phe-371 and Leu-405 of SARS-CoV-2 spike glycoprotein	−7.27	Schrodinger maestro	[38]
Saikosaponin K $C_{54}H_{88}O_{22}$	Spike protein PDB ID:6VSB	Inhibition	Saikosaponin K forms a hydrogen bond with Phe-403, Ser-402, Glu-404 and Asp-345 while binding with SARS-CoV-2 spike glycoprotein and interacts hydrophobically with Tyr-313, Leu-342, Pro-343, Phe-346, Pro-370, Phe-371, Phe-403 and Leu-405 while binding with SARS-CoV-2 spike glycoprotein	−6.25	Schrodinger maestro	[38]
Saikosaponin U $C_{59}H_{96}O_{29}$	Spike protein PDB ID:6VSB	Inhibition	Saikosaponin U forms a hydrogen bond with amino acid residues, namely, Phe-346, Ser-402, Asn-271, Glu-257 and Asp-345 while binding with SARS-CoV-2 spike glycoprotein. It also exhibits hydrophobic interaction with Trp-270, Pro-343, Phe-346, Gly-348, Phe-403, Leu-405, Phe-371 and Tyr-313 of SARS-CoV-2 spike glycoprotein	-8.42	Schrodinger maestro	[38]
Saikosaponin V $C_{53}H_{86}O_{24}$	Spike protein PDB ID:6VSB	Inhibition	Saikosaponin V forms a hydrogen bond with Phe-346, Ser-402, Thr-460, Ile-475, Asp-459, Thr-461, Phe-403 and Gly-298 while binding with SARS-CoV-2 spike glycoprotein. It also exhibits hydrophobic interaction with Val-299, Leu-307, Phe-346, Phe-403, Leu-405, Phe-429, Leu-434, Ile-475 and Pro-477 of SARS-CoV-2 spike glycoprotein	−8.29	Schrodinger maestro	[38]

Table 1 (continued)

Name of compound	Targeted protein/enzyme	Nature of interaction	Molecular interactions	Binding energy (kcal/mol) or docking score	Software utilized	References
Tenufolin $C_{36}H_{56}O_{12}$	Spike Protein PDB ID:6LZG	Inhibition	Tenuifolin forms a hydrogen bond with Leu-A:73, Asp-A:350 and Tyr:A-385, Asn-A:394 and interacts via hydrophobic bond with amino acid residues, namely, Phe-A:390, Leu-A:73	− 8.7	Autodock Tool	[47]
Ursolic acid $C_{30}H_{48}O_3$	Spike protein PDB ID:6VYB	Inhibition	While binding with SARS-Cov-2 spike protein, ursolic acid generates hydrogen bonds with His-1058 and Leu-861	− 89.94	iGEMDOCK	[24]
Zingerone $C_{11}H_{14}O_3$	Spike protein PDB ID:6VYB	Inhibition	Zingerone exhibits hydrogen bonds with amino acid residues, namely, Asn-978, Arg-1000, Thr-573, Tyr-741 and Gly-744 while binding with SARS-CoV-2 spike protein	− 102.18	iGEMDOCK	[24]

astragalin (− 9.12 kcal/mol); and calendoflaside (− 8.5 kcal/mol) [26–30]. Eventually, data which are available in the literature revealed that some synthetic drugs that showed promising role against SARS-CoV-2 by inhibiting M^{pro} are carfilzomib (− 13.8 kcal/mol), azithromycin (− 8.2 kcal/mol), chloroquine (− 7.9 kcal/mol), hydroxychloroquine (− 6.5 kcal/mol), streptomycin (− 3.8 kcal/mol), and ribavirin (− 2.01 kcal/mol) [31]. Contrary to our findings, it can be predicted that the phytoconstituents reported in this current review may also show a promising role against SARS-CoV-2 inhibition, as compared to that of the synthetic ones. However, as mentioned in the earlier statement, there is a lack of research in in vivo models which may be regarded as a research gap and need to be evaluated further. However, a further check-in drug-likeness for calendoflaside using the Molsoft database (www.molsoft.com/mprop/) suggested that there were three penalties of Lipin's key rule of 5 with molecular weight, 608.17 (> 500); number of hydrogen bond acceptor (HBA), 15 (> 10); and number of hydrogen bond donor (HBD), 8(> 5). Cryptospirolepine has two penalties with molecular weight 504.20 (> 500) and mol LogP 5.98 (> 5). Acetoside showed three penalties with molecular weight, 624.21(> 500); number of HBA, 15(> 10); and number of HBD, 9(> 5). The above findings show a major research gap with no studies designed to enhance the drug-likeness of the above phytoconstituents. A chemical modification can be done on acetoside, cryptospirolepine, and calenoflaside to eliminate the drug-likeness penalties. Hence, it can be inferred that laurolistine, avicularin, astragalin, and cryptoquindoline (Fig. 3) can be potent phytoconstituents against SARS-CoV-2 by inhibiting M^{pro}.

Binding affinity of phytoconstituents with ACE-2 of host cell receptor

A total of 6 phytoconstituents were found to act on the ACE-2 target. Out of which, absinthin has the docking score of − 11.8 kcal/mol followed by 3,5-di-O-galloylshikimic acid (− 10 kcal/mol), scutellarein 7-glucoside (− 9.3 kcal/mol), avicularin (− 8.0 kcal/mol), cirsimaritin (− 7.2 kcal/mol), and hispidulin (− 7.3 kcal/mol) [30, 32, 33]. Some of the synthetic drugs targeting ACE-2 in host cells are azithromycin (− 10.5 kcal/mol), hydroxychloroquine (− 8.5 kcal/mol), and chloroquine (− 4.2 kcal/mol) [31]. This implies that absinthin, 3,5-di-O-galloylshikimic acid, scutellarein 7-glucoside, avicularin, cirsimaritin, and hispidulin have a nearly identical binding score to the synthetic medication that targets ACE-2. It is possible that such phytoconstituents may demonstrate the promising binding activity with ACE-2 and hence will play a role in SARS-CoV-2 suppression. However, a check-in drug-likeness for scutellarein 7-glucoside using the Molsoft database (www.molsoft.com/mprop/) suggested that there were two penalties of Lipin's key rule of 5 with a number of HBA 11(> 10) and number of HBD 7(> 5). On the other

Table 2 Binding probability of diverse classes of phytochemicals against different site proteins of SARS-CoV-2

Phytochemical class	M-Pro	S-Protein	ACE-2	PL-pro	E	S-RBD	NSP15-endoribonuclease	RdRp
Flavonoids	14	6	4	0	1	0	0	0
Coumarin	18	1	0	0	0	0	0	0
Alkaloid	12	0	0	0	0	0	0	0
Steroids (tetracyclic and pentacyclic)	10	7	0	1	0	1	5	1
Phenolic	6	4	0	0	0	0	0	0
Tannin	6	2	1	0	0	0	0	0
Glycoside	4	2	0	0	0	2	1	0
Triterpenoid	4	0	1	0	2	0	0	0
Miscellaneous	3	1	0	0	0	0	0	0
Total	77	23	6	1	3	3	6	1

hand, there was no preclinical or clinical study conducted on absinthin, 3,5-di-O-galloylshikimic acid, avicularin, cirsimaritin, and hispidulin to determine its effect on SARS-CoV-2 creating a major gap in research. The structure of phytoconstituents inhibiting ACE-2 and with no penalties of Lipin's key rule of 5 is shown in Fig. 4.

Binding affinity of phytoconstituents with RdRp

Some of the synthetic drugs that inhibit the enzyme RdRp with best binding energy are raltegravir (−9.5 kcal/mol), doxazosin (−9.3 kcal/mol), tadalafil (−9.2 kcal/mol), and ceftriaxone (−9.0 kcal/mol) [34]. According to the current review, one phytoconstituent, namely, asparoside-C binds to RdRp with a binding energy of −6.65 kcal/mol [35]. Moreover, a check-in drug-likeness for asparoside-C using the Molsoft database (www.molsoft.com/mprop/) suggested that there were 3 penalties of Lipin's key rule of 5 with molecular weight 1212.61 (> 500), a number of HBA 27 (> 10), and number of HBD 15 (> 5). However, asparoside-C can still be chemically modified to get rid of the penalties of Lipin's key rule of 5 and approached for further studies to treat SARS-CoV-2.

Table 3 Phytoconstituents showing better stability with targets of SARS-CoV-2 based on their binding energy

Name of compound	Target protein	Binding energy (k/cal)	Reference
Laurolistine	M^{pro}	−294.15	[26]
Curcumin	Spike protein	−115.198	[24]
Apigenin	Spike protein	−108.614	[24]
Chrysophanol	Spike protein	−107.385	[24]
Emodin	Spike protein	−105.462	[24]
Zingerone	Spike protein	−102.18	[24]
Gingerol	Spike protein	−98.03	[24]
Epigallocatechin gallate	Spike protein	−91.72	[24]
Ursolic acid	Spike protein	−89.94	[24]
Ajoene	Spike protein	−74.2819	[24]

Binding affinity of phytoconstituents with receptor binding domain of spike protein (S-RBD)

The phytoconstituents that bind to S-RBD are asparoside-C (−7.16 kcal/mol), asparoside-D (−7.06 kcal/mol), and shatavarin-I (−6.52 kcal/mol) [35]. Literature reports that some well-known synthetic drugs that bind to S-RBD are azithromycin (−7.0 kcal/mol), chloroquine (−4.2 kcal/mol), and hydroxychloroquine (−4.9 kcal/mol) [31]. This suggests that asparoside-C, asparoside-D, and shatavarin-I probably have similar binding energy when compared to the synthetic drug. However, a check-in drug-likeness for asparoside-C using the Molsoft database (www.molsoft.com/mprop/) suggested that there were three penalties of Lipin's key rule of 5 with molecular weight 1212.61 (> 500), number of HBA 27 (> 10), and number of HBD 15 (> 5). Asparoside-D showed three penalties with molecular weight 1198.60 (> 500), number of HBA 27 (> 10), and number of HBD: 16 (> 5). Similarly, Shatavarin-I also showed 3 penalties of Lipin's key rule of 5 with molecular weight 1066.56 (> 500), number of HBA 23 (> 10), and number of HBD 14 (> 5). Therefore, all three phytoconstituents must be chemically modified in the future for further studies to treat SARS-CoV-2.

Binding affinity of phytoconstituents with E protein

As per the literature, we found 3 phytoconstituents that act on the E protein target, viz., belachinal (−11.46 kcal/mol), macaflavanone E (−11.07 kcal/mol), and vibsanol B (−11.01 kcal/mol) [36]. Moreover, some of the synthetic antiviral drugs that bind to E protein include glecaprevir (−11.8 kcal/mol), saquinavir (−10.7 kcal/mol), and simeprevir (−11.3 kcal/mol) [37]. This suggests that belachinal binding energy towards E protein is more or less similar

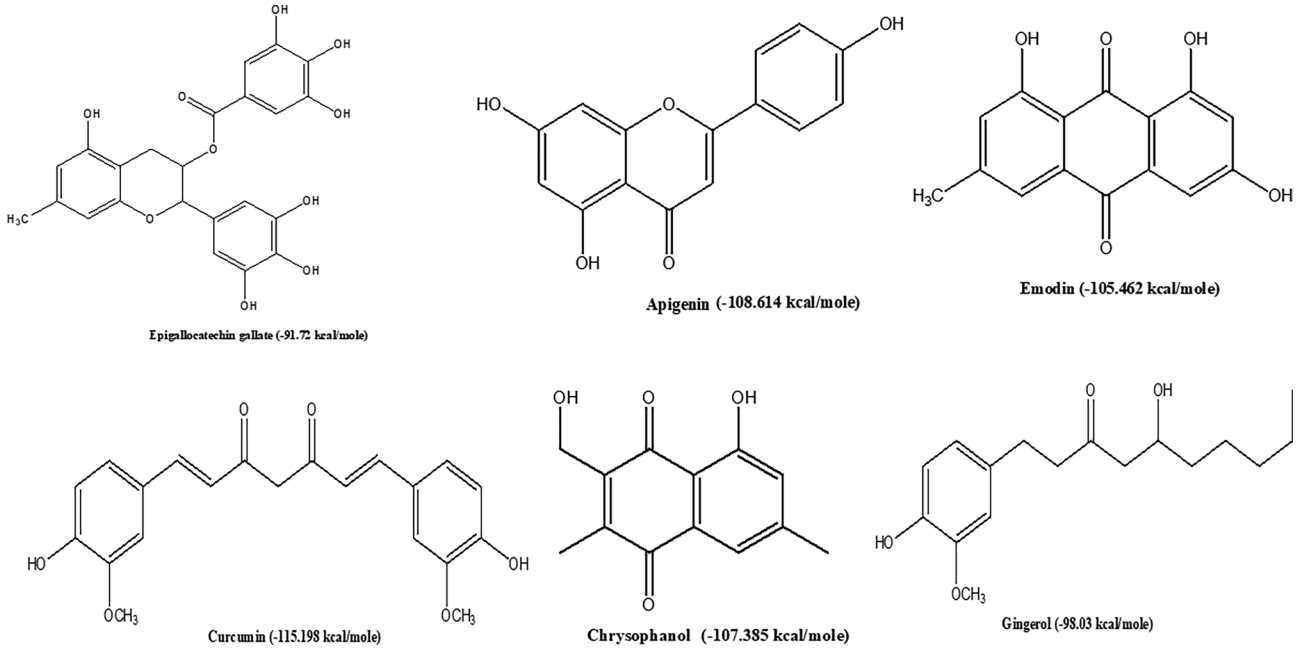

Fig. 2 Phytoconstituents inhibiting spike glycoprotein and their binding energy

to that of the reported synthetic drugs. However, a check-in drug-likeness for belachinal using Molsoft database (www.molsoft.com/mprop/) suggested that there is only one penalty of Lipin's key rule of 5 with mol logP 5.78 (> 5). Therefore, the phytoconstituents like belachinal can be chemically modified and approached for studying anti-SARS-CoV-2 properties. In addition, compounds like macaflavanone E and vibsanol B (Fig. 5) have similar

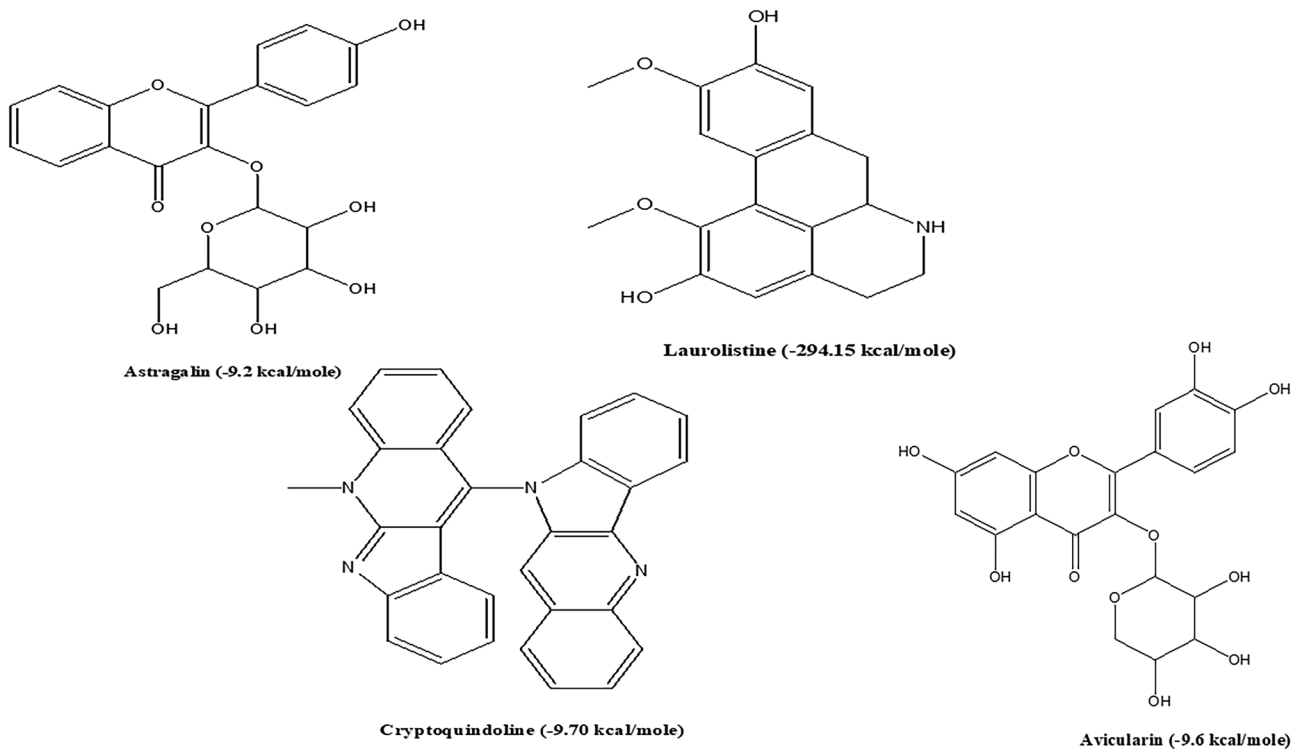

Fig. 3 Phytoconstituents inhibiting M^{pro} and their binding energy

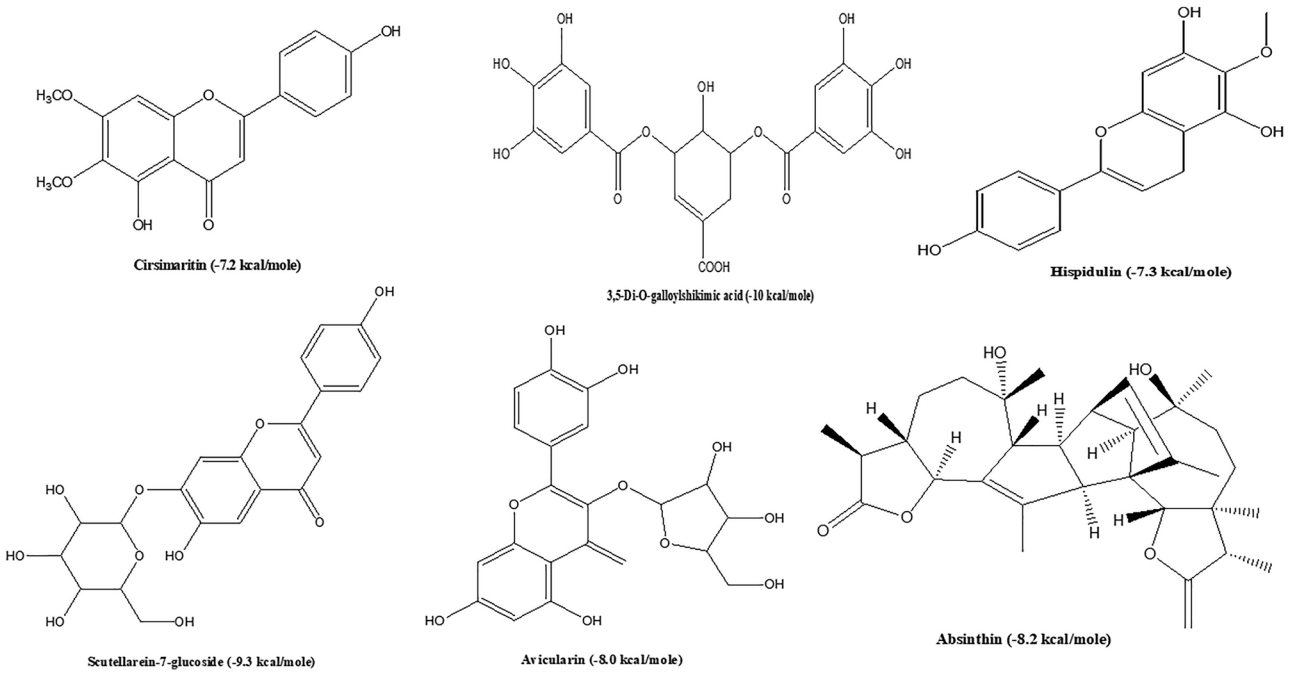

Fig. 4 Phytoconstituents inhibiting ACE-2 and their binding energy

binding energy to synthetic drugs that bind to E protein. Moreover, it passes the drug-likeness. However, there was no evidence of its preclinical or clinical studies to determine its effect on SARS-CoV-2, creating a major gap in research. Hence, macaflavanone E and vibsanol B can be further explored for their effect on SARS-CoV-2.

Binding affinity of phytoconstituents with NSP-15 endoribonuclease

Based on the information collected in the literature, a total of 6 phytoconstituents were discovered to bind to the NSP15-endoribonuclease target. According to reports, saikosaponin V, saikosaponin U, saikosaponin K, saikosaponin C, asparoside-D, and asparoside-C all effectively bind to NSP15-endoribonuclease with binding energies of − 8.35 kcal/mol, − 7.27 kcal/mol, − 6.79 kcal/mol, − 6.98 kcal/mol, − 6.44 kcal/mol, and − 7.54 kcal/mol, respectively [35, 38]. Meanwhile, investigations on synthetic drugs with comparable protein targets have been published in the literature, including ceftolozane (− 7.83 kcal/mol), azacitidine (− 6.74 kcal/mol), saquinavir (− 5.76 kcal/mol), and amikacin (− 5.69 kcal/mol) [39]. A drug-likeness assessment utilizing the Molsoft database (www.molsoft.com/mprop/) revealed that saikosaponin V displayed three penalties of Lipin's main rule of 5 with molecular weight 1106.55 (> 500), number of HBA 24 (> 10), and number of HBD 16 (> 5). Saikosaponin U exhibited three penalties: molecular weight of 1268.60 > 500, a number of HBA of 29 > 10, and a number of HBD of 19 > 5. Similarly, asparoside-D was penalized with three penalties (molecular weight 1198.60 (> 500), number of HBA 27 (> 10), and number of HBD 16 (> 5)) and asparoside-C with molecular weight 1212.61 (> 500), number of HBA 27 (> 10), and number of HBD 15 (> 5) displayed three penalties of Lipin's fundamental rule of 5. However, because saikosaponin V has higher binding effectiveness than synthetic medicines, it can be chemically manipulated and used to combat SARS-CoV-2.

Binding affinity of phytoconstituents with PL.pro of SARS-CoV-2

According to the current review, asparoside-C was the sole phytoconstituent with a binding energy of − 5.44 kcal/mol with PL^{pro} [35]. Levofloxacin (− 6.8 kcal/mol), dexamethasone (− 6.5 kcal/mol), ciprofloxacin (− 6.1 kcal/mol), and chloroquine (− 5.3 kcal/mol) are some synthetic drugs that bind to the same protein [40]. This essentially implies that phytoconstituents such as asparoside-C might be a viable source of medicines that act on PL^{pro}. However, a check-in drug-likeness for asparoside-C using the Molsoft database (www.molsoft.com/mprop/) suggested that there were three penalties of Lipin's key rule of 5 with molecular weight 1212.61 (> 500), number of HBA 27 (> 10), and number of HBD 15 (> 5). Although asparoside-C has less binding efficacy than the marketed drugs, it is always wise to further study the anti-SARS-CoV-2 activity with some chemical modification.

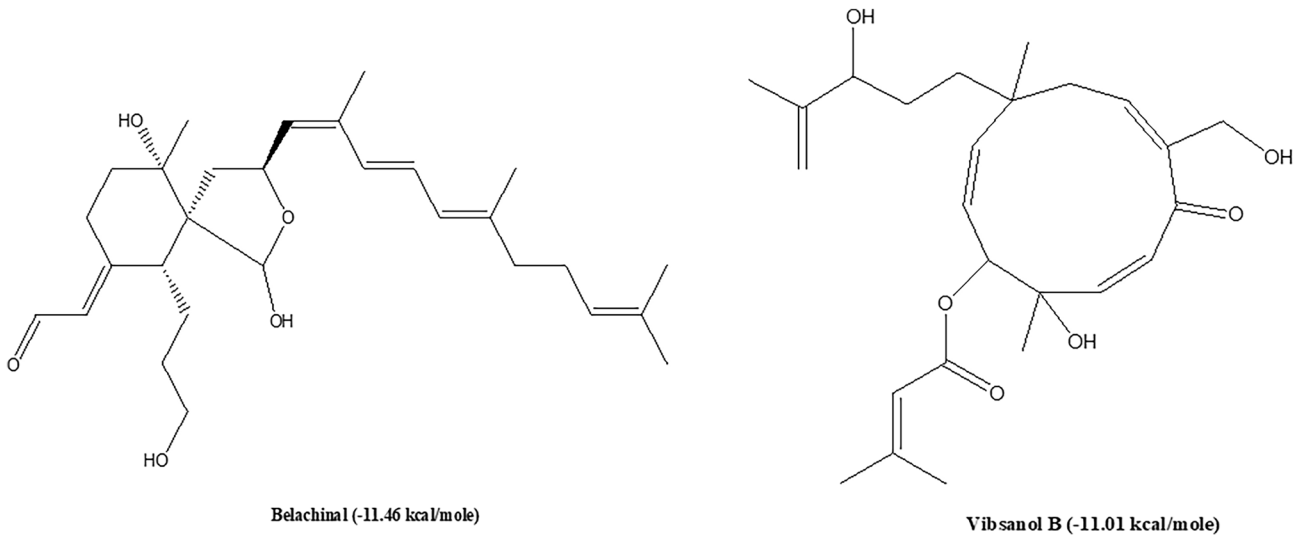

Fig. 5 Phytoconstituents inhibiting E protein and their binding energy

Discussion and conclusion

It has been almost a year and a half since the people of the world have been suffering from the infection caused by SARS-CoV-2. It has resulted in an increased incidence of mortality and economic failure. Despite discovering new antiviral drugs, biological products, and potential vaccines to reduce the virus's activity, people continue to be victims of this deadly virus. Moreover, due to the emergence of new variants that results from rapid mutation change, the virus tends to change its conformation quickly and infect the host more prominently. Based on the increased prevalence of the new COVID-19 variants, scientists have been investigating a plethora of drugs that may be repurposed to fight COVID-19 and many of these drugs are producing severe drug interaction and unwanted side effects. Azithromycin, heparin, and some synthetic drugs like hydroxychloroquine, chloroquine, clozapine, ritonavir, and atazanavir are commonly used to manage COVID-19 severe side effects that affect the hematopoietic system and the cardiovascular system [52]. As discussed earlier, plants and their natural components might have lesser side effects and can potentially reduce the SARS-CoV-2 severity and complexity. In this context, based on the available information reported by various researchers, the current review elaborated on the in silico studies on the inhibiting efficacy of a total of 100 active constituents from plant sources which can be future promising agents to fight against SARS-CoV-2. From the critical findings as represented in Fig. 6, it was observed that the majority of the phytochemical class that effectively binds with the active protein sites of SARS-CoV-2 are flavonoids (20%), coumarins (18%), steroids (18%), and to the lesser extent alkaloids (12%). Interestingly, it was observed that approximately 70% of the active phytochemical constituents (including laurolistine) were shown to bind successfully with the viral for main protease (M^{pro}) and to a lesser amount with the spike protein and other proteins associated with COVID-19 (Tables 2 and 3). As a result, M^{pro} might be a possible place for scientists to target medications in order to block or diminish SARS-CoV-2 activity. 7

The bioactive phytoconstituents (alkaloids, flavonoids, glucosinolates, phenolics) are repurposed as prospective platforms for anti-SARS-CoV-2 therapies. The present investigations reveal that virtual screening has recently repurposed many phytochemicals such as COVID-19 M^{pro}. They have mainly bound with the 3-chymotrypsin-like

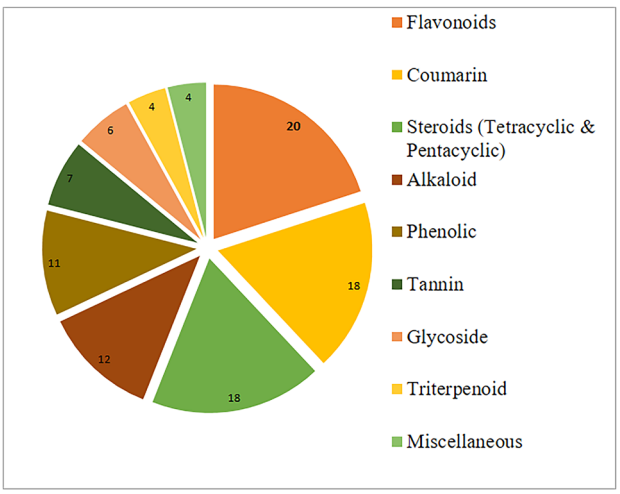

Fig. 6 Diversity of active phytoconstituents binding to SARS-CoV-2 target proteins

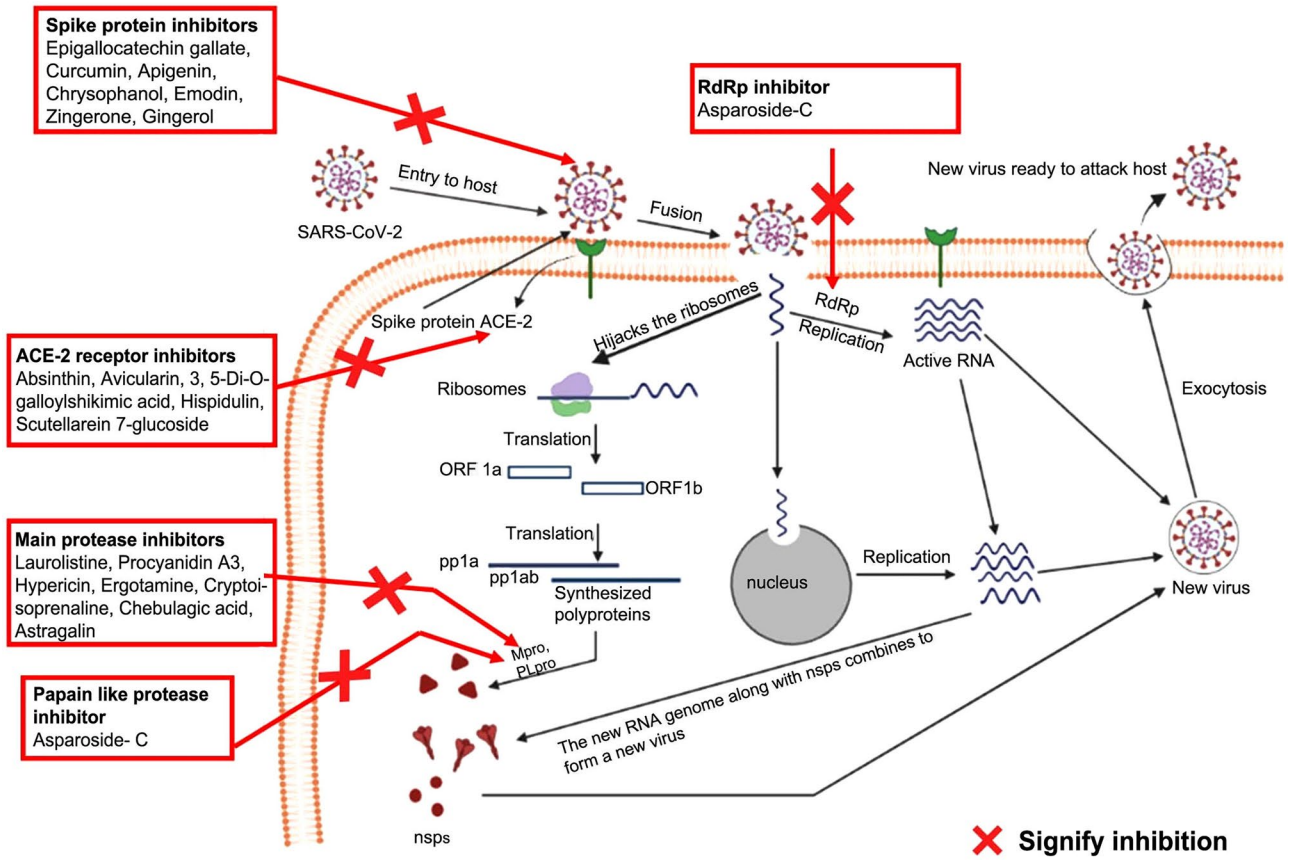

Fig. 7 A summary of the phytoconstituents acting on different targets of SARS-CoV-2

(3CLpro) and papain-like proteases (PL^{pro}), spike glycoprotein, ACE-2, NSP15-endoribonuclease, and E protein targets of SARS-CoV-2 main protease using in silico molecular docking approach. From the current review analysis, it was further observed that different classes of phytoconstituents act at different active sites of the virus (Fig. 7); this includes the following plant metabolites: (a) curcumin, apigenin, quercetin, colchicine, piperine, caffeic acid, chrysophanol, emodin, zingerone, gingerol, and epigallocatechin gallate are significantly binding with spike glycoprotein; (b) laurolistine, acetoside, cryptoquindoline, avicularin, cryptospirolepine, astragalin, and calendoflaside are bound with M^{pro}; (c) absinthin, 3,5-di-O-galloylshikimic acid, avicularin, cirsimaritin, and hispidulin bind to the ACE-2 target; and (d) macaflavanone E and vibsanol B bind to E protein.

Much of the research gaps were observed from the current review, which may theoretically be regarded as legitimate information for additional exploration by researchers globally. Finally, it is important to identify any key research gaps that resulted from the findings of the current assessment for future perspectives. Such critical gaps include the following: (a) most of the phytoconstituents which were reported in the current review required chemical modification as per the information obtained from drug-likeliness screening; (b) secondly, the data which is reported in the literature solely deals with the virtual screening of phytoconstituents for SARS-CoV-2 inhibition. These research gaps can be critically ascertained and minimized if the studies of the phytoconstituents were done in in vivo models followed by clinical evaluation. In silico data supported in vivo studies; (c) finally, in addition to the 100 phytoconstituents presented in this research, there is a need to delve deeper into new phytoconstituents for probable viral inhibition. This will have a significant influence on encouraging the use of natural items for the treatment of COVID-19-related medical problems.

Acknowledgements We would like to acknowledge the Girijananda Chowdhury Institute of Pharmaceutical Sciences, Guwahati-781017, Assam, India.

Author contribution SK, IH, DL, SK, JMK, and HS have equally contributed to the work.

Data availability The datasets generated during and or analyzed during the study are available with the corresponding author.

Declarations

Conflict of interest The authors declare no competing interests.

References

1. Korber B, Fischer WM, Gnanakaran S, Yoon H, Theiler J et al (2020) Tracking changes in SARS-CoV-2 spike: evidence that D614G increases infectivity of the COVID-19 virus. Cell 182:812–827. https://doi.org/10.1016/j.cell.2020.06.043
2. Russo M, Moccia S, Spagnuolo C, Tedesco I, Russo GL (2020) Roles of flavonoids against coronavirus infection. Chem -Biol Interact 328:1–13. https://doi.org/10.1016/j.cbi.2020.109211
3. Zhu N, Zhang D, Wang W, Li X, Yang B et al (2020) A novel coronavirus from patients with pneumonia in China, 2019. N Engl J Med 382:727–733. https://doi.org/10.1056/nejmoa2001017
4. WHO (2022) WHO Coronavirus (COVID-19) Dashboard. https://covid19.who.int/table. Accessed 20 April 2022
5. Forni C, Facchiano F, Bartoli M, Pieretti S, Facchiano A et al (2019) Beneficial role of phytochemicals on oxidative stress and age-related diseases. BioMed Res Int 8748253:1–16. https://doi.org/10.1155/2019/8748253
6. Hazarika I, Mukundan GK, Sundari PS, Laloo D (2021) Journey of *Hydrocotyle sibthorpioides* Lam.: From traditional utilization to modern therapeutics—a review. Phytother Res 35:1847–1871. https://doi.org/10.1002/ptr.6924
7. Tiwari S (2008) Plants: a rich source of herbal medicine. J Nat Prod 1:27–35. https://www.researchgate.net/publication/266049813_Plants-herbs_wealth_as_a_potential_source_of_ayurvedic_drugs
8. Bhuiyan FR, Howlader S, Raihan T, Hasan M (2020) Plants metabolites: possibility of natural therapeutics against the COVID-19 pandemic. Front Biomed 7:1–26. https://doi.org/10.3389/fmed.2020.00444
9. Selçuk AA (2019) A guide for systematic reviews: PRISMA. Turk Arch Otorhinolaryngol 57:57. https://doi.org/10.5152/tao.2019.4058
10. Astuti I (2020) Severe acute respiratory syndrome coronavirus 2 (SARS-CoV-2): an overview of viral structure and host response. Diabetes Metab Syndr Clin Res Rev 14:407–412. https://doi.org/10.1016/j.dsx.2020.04.020
11. Liu YC, Kuo RL, Shih SR (2020) COVID-19: the first documented coronavirus pandemic in history. Biomed J 43:328–333. https://doi.org/10.1016/j.bj.2020.04.007
12. Kumar S, Nyodu R, Maurya VK, Saxena SK (2020) Morphology, genome organization, replication, and pathogenesis of severe acute respiratory syndrome coronavirus 2 (SARS-CoV-2). Springer, Singapore. https://doi.org/10.1007/978-981-15-4814-7_3
13. J Alsaadi EA, Jones IM (2019) Membrane binding proteins of coronaviruses. Future Virol 14:275–286. https://doi.org/10.2217/fvl-2018-0144
14. Neuman BW, Kiss G, Kunding AH, Bhella D, Baksh MF et al (2011) A structural analysis of M protein in coronavirus assembly and morphology. J Struct Biol 174:11–22. https://doi.org/10.1016/j.jsb.2010.11.021
15. Schoeman D, Fielding BC (2019) Coronavirus envelope protein: current knowledge. Virol J 16:1–22. https://doi.org/10.1186/s12985-019-1182-0
16. Khattari Z, Brotons G, Akkawi M, Arbely E, Arkin IT, Salditt T (2006) SARS coronavirus E protein in phospholipid bilayers: an x-ray study. Biophys J 90:2038–2050. https://doi.org/10.1529/biophysj.105.072892
17. Duart G, García-Murria MJ, Grau B, Acosta-Cáceres JM, Martínez-Gil L et al (2020) SARS-CoV-2 envelope protein topology in eukaryotic membranes. Open Biol 10:200209. https://doi.org/10.1101/2020.05.27.118752
18. Ruch TR, Machamer CE (2012) The coronavirus E protein: assembly and beyond. Viruses 4:363–382. https://doi.org/10.3390/v4030363
19. Venkatagopalan P, Daskalova SM, Lopez LA, Dolezal KA, Hogue BG (2015) Coronavirus envelope (E) protein remains at the site of assembly. Virology 478:75–85. https://doi.org/10.1016/j.virol.2015.02.005
20. Laude H, Masters PS (1995) The Coronavirus Nucleocapsid Protein. In Siddell SG (eds) The Coronaviridae. The Viruses. Springer, Boston, MA. https://doi.org/10.1007/978-1-4899-1531-3_7
21. Kang S, Yang M, Hong Z, Zhang L, Huang Z et al (2020) Crystal structure of SARS-CoV-2 nucleocapsid protein RNA binding domain reveals potential unique drug targeting sites. Acta Pharmaceutica Sinica 10:1228–1238. https://doi.org/10.1016/j.apsb.2020.04.009
22. Dutta NK, Mazumdar K, Gordy JT (2020) The nucleocapsid protein of SARS–CoV-2: a target for vaccine development. J Virol 94:1–2. https://doi.org/10.1128/jvi.00647-20
23. Pinzi L, Rastelli G (2019) Molecular docking: shifting paradigms in drug discovery. Int J Mol Sci 20:1–23. https://doi.org/10.3390/ijms20184331
24. Subbaiyan A, Ravichandran K, Singh SV, Sankar M, Thomas P et al (2020) In silico molecular docking analysis targeting SARS-CoV-2 spike protein and selected herbal constituents. J Pure Appl Microbiol 14: 989–998. https://doi.org/10.22207/JPAM.14.SPL1.37
25. Toor HG, Banerjee DI, Rath SL, Darji SA (2021) Computational drug repurposing targeting the spike glycoprotein of SARS-CoV-2 as an effective strategy to neutralize COVID-19. Eur J Pharmacol 890:1–17. https://doi.org/10.1016/j.ejphar.2020.173720
26. Kumar N, Singh A, Gulati HK, Bhagat K, Kaur K et al (2021) Phytoconstituents from ten natural herbs as potent inhibitors of main protease enzyme of SARS-COV-2: in silico study. Phytomedicine Plus 1:1–13. https://doi.org/10.1016/j.phyplu.2021.100083
27. Gyebi GA, Ogunro OB, Adegunloye AP, Ogunyemi OM, Afolabi SO (2021) Potential inhibitors of coronavirus 3-chymotrypsin-like protease (3CLpro): an in silico screening of alkaloids and terpenoids from African medicinal plants. J Biomol Struct Dyn 39:3396–3408. https://doi.org/10.1080/07391102.2020.1764868
28. Das P, Majumder R, Mandal M, Basak P (2021) In-Silico approach for identification of effective and stable inhibitors for COVID-19 main protease (Mpro) from flavonoid based phytochemical constituents of *Calendula officinalis*. J Biomol Struct Dyn 39:6265–6280. https://doi.org/10.1080/07391102.2020.1796799
29. Teli DM, Shah MB, Chhabria MT (2021) In silico screening of natural compounds as potential inhibitors of SARS-CoV-2 main protease and spike RBD: targets for COVID-19. Front Mol Biosci 7:1–25. https://doi.org/10.3389/fmolb.2020.599079
30. Sharma P, Shanavas A (2021) Natural derivatives with dual binding potential against SARS-CoV-2 main protease and human ACE2 possess low oral bioavailability: a brief computational analysis. J Biomol Struct Dyn 39:5819–5830. https://doi.org/10.1080/07391102.2020.1794970
31. Braz HLB, de Moraes Silveira JA, Marinho AD, de Moraes MEA, de Moraes Filho MO et al (2020) In silico study of azithromycin, chloroquine and hydroxychloroquine and their potential mechanisms of action against SARS-CoV-2 infection. Int J Antimicrob Agents 56:1–8. https://doi.org/10.1016/j.ijantimicag.2020.106119
32. Joshi T, Joshi T, Sharma P, Mathpal S, Pundir H et al (2020) In silico screening of natural compounds against COVID-19 by

targeting Mpro and ACE2 using molecular docking. Eur Rev Med Pharmacol Sci 24:4529–4536. https://doi.org/10.26355/eurrev_202004_21036
33. Omar S, Bouziane I, Bouslama Z, Djemel A (2020) In-silico identification of potent inhibitors of COVID-19 main protease (Mpro) and angiotensin converting enzyme 2 (ACE2) from natural products: quercetin, hispidulin, and cirsimaritin exhibited better potential inhibition than hydroxy-chloroquine against COVID-19 main protease active site and ACE2. https://doi.org/10.26434/chemrxiv.12181404.v1
34. Molavi Z, Razi S, Mirmotalebisohi SA, Adibi A, Sameni M et al (2021) Identification of FDA approved drugs against SARS-CoV-2 RNA dependent RNA polymerase (RdRp) and 3-chymotrypsin-like protease (3CLpro), drug repurposing approach. Biomed Pharmacother 138:1–20. https://doi.org/10.1016/j.biopha.2021.111544
35. Chikhale RV, Sinha SK, Patil RB, Prasad SK, Shakya A et al (2021) In-silico investigation of phytochemicals from Asparagus racemosus as plausible antiviral agent in COVID-19. J Biomol Struct Dyn 39: 5033–5047. https://doi.org/10.1080/07391102.2020.1784289
36. Gupta MK, Vemula S, Donde R, Gouda G, Behera L et al (2021) In-silico approaches to detect inhibitors of the human severe acute respiratory syndrome coronavirus envelope protein ion channel. J Biomol Struct Dyn 39:2617–2627. https://doi.org/10.1080/07391102.2020.1751300
37. Chernyshev A (2020) Pharmaceutical targeting the envelope protein of SARS-CoV-2: the screening for inhibitors in approved drugs. https://doi.org/10.26434/chemrxiv.12286421.v1
38. Sinha SK., Shakya A, Prasad SK, Singh S, Gurav NS et al (2021) An in-silico evaluation of different Saikosaponins for their potency against SARS-CoV-2 using NSP15 and fusion spike glycoprotein as targets. J Biomol Struct Dyn 39:3244–3255. https://doi.org/10.1080/07391102.2020.1762741
39. Shaik A, Natarajan N, Kirubakaran S, Thiruvenkatam V (2020) Virtual screening of FDA approved drugs against Nsp15 endoribonuclease from SARS CoV-2. https://doi.org/10.26434/chemrxiv.13265519.v1
40. Marciniec K, Beberok A, Boryczka S, Wrześniok D (2021) The application ofin silico experimental model in the assessment of ciprofloxacin and levofloxacin interaction with main SARS-CoV-2 targets: S-, E-and TMPRSS2 proteins, RNA-dependent RNA polymerase and papain-like protease (PLpro)—preliminary molecular docking analysis. Pharmacol Rep 73:1765–1780. https://doi.org/10.1007/s43440-021-00282-8
41. Cetin A (2021) In silico studies on stilbenolignan analogues as SARS-CoV-2 Mpro inhibitors. Chem Phys Lett 771:1–9. https://doi.org/10.1016/j.cplett.2021.138563
42. Lyndem S, Sarmah S, Das S, Roy AS (2020) In silico screening of naturally occurring coumarin derivatives for the inhibition of the main protease of SARS-CoV-2. https://doi.org/10.26434/chemrxiv.12234728
43. Islam R, Parves MR, Paul AS, Uddin N, Rahman MS et al (2021) A molecular modeling approach to identify effective antiviral phytochemicals against the main protease of SARS-CoV-2. J Biomol Struct Dyn 39:3213–3224. https://doi.org/10.1080/07391102.2020.1761883
44. Krupanidhi S, Abraham Peele K, Venkateswarulu TC, Ayyagari VS, Nazneen Bobby M et al (2021) Screening of phytochemical compounds of *Tinospora cordifolia* for their inhibitory activity on SARS-CoV-2: an in silico study. J Biomol Struct Dyn 39:5799–5803. https://doi.org/10.1080/07391102.2020.1787226
45. Bouchentouf S, Missoum N (2020) Identification of compounds from *Nigella Sativa* as new potential inhibitors of 2019 novel coronavirus (Covid-19): molecular docking study. https://doi.org/10.20944/preprints202004.0079.v1
46. Shah B, Shree Devi MS, Narayanan K (2020) Repurposing of Medicinal plants used in Siddha formulations as Potential Protease Inhibitors of COVID-19: an in silico approach. https://doi.org/10.2139/ssrn.3650390
47. Prasanth DSNBK, Murahari M, Chandramohan V, Panda SP, Atmakuri LR et al (2021a) In silico identification of potential inhibitors from Cinnamon against main protease and spike glycoprotein of SARS CoV-2. J Biomol Struct Dyn 39:4618–4632. https://doi.org/10.1080/07391102.2020.1779129
48. Gurung AB, Ali MA, Lee J, Farah MA, Al-Anazi KM (2020) In silicoscreening of FDA approved drugs reveals ergotamine and dihydroergotamine as potential coronavirus main protease enzyme inhibitors. Saudi J Biol Sci 27:2674–2682. https://doi.org/10.1016/j.sjbs.2020.06.005
49. Pandey P, Rane JS, Chatterjee A, Kumar A, Khan R et al (2021) Targeting SARS-CoV-2 spike protein of COVID-19 with naturally occurring phytochemicals: an in silico study for drug development. J Biomol Struct Dyn 39:6306–6316. https://doi.org/10.1080/07391102.2020.1796811
50. Prasanth DSNBK, Murahari M, Chandramohan V, Bhavya G, Lakshmana Rao A et al (2021b) In-silico strategies of some selected phytoconstituents from *Melissa officinalis* as SARS CoV-2 main protease and spike protein (COVID-19) inhibitors. Mol Simul 47:457–470. https://doi.org/10.1080/08927022.2021.1880576
51. Chandel V, Raj S, Rathi B, Kumar D (2020) In silico identification of potent COVID-19 main protease inhibitors from FDA approved antiviral compounds and active phytochemicals through molecular docking: a drug repurposing approach. https://doi.org/10.20944/preprints202003.0349.v1
52. Aygün İ, Kaya M, Alhajj R (2020) Identifying side effects of commonly used drugs in the treatment of Covid 19. Sci Rep 10:1–14. https://doi.org/10.1038/s41598-020-78697-1